CAPITAL UNIVERSITY OF SCIENCE AND
TECHNOLOGY, ISLAMABAD

Acoustic Scattering in Flexible Bifurcated Cylindrical Waveguide

by

Aqsa Shaheen

A thesis submitted in partial fulfillment for the
degree of Master of Philosophy

in the

Faculty of Computing
Department of Mathematics

2019

Dedicated to my beloved brothers **Ikhlaq Ahmed** and **Shahzad Ahmed**
without their efforts and support, I could never do this.

CERTIFICATE OF APPROVAL

Acoustic Scattering in Flexible Bifurcated Cylindrical Waveguide

by

Aqsa Shaheen

(MMT171022)

THESIS EXAMINING COMMITTEE

S. No.	Examiner	Name	Organization
(a)	External Examiner	Dr. Muhammad Ayub	QAU, Islamabad
(b)	Internal Examiner	Dr. Rashid Ali	CUST, Islamabad
(c)	Supervisor	Dr. Muhammad Afzal	CUST, Islamabad

Thesis Supervisor
Dr. Muhammad Afzal
September, 2019

Author's Declaration

I, **Aqsa Shaheen** hereby state that my M.Phil thesis titled "**Acoustic Scattering in Flexible Bifurcated Cylindrical Waveguide** " is my own work and has not been submitted previously by me for taking any degree from Capital University of Science and Technology, Islamabad or anywhere else in the country/abroad.

At any time if my statement is found to be incorrect even after my graduation, the University has the right to withdraw my M.Phil Degree.

(Aqsa Shaheen)

Registration No: MMT171022

Plagiarism Undertaking

I solemnly declare that research work presented in this thesis titled "**Acoustic Scattering in Flexible Bifurcated Cylindrical Waveguide**" is solely my research work with no significant contribution from any other person. Small contribution/help wherever taken has been dully acknowledged and that complete thesis has been written by me.

I understand the zero tolerance policy of the HEC and Capital University of Science and Technology towards plagiarism. Therefore, I as an author of the above titled thesis declare that no portion of my thesis has been plagiarized and any material used as reference is properly referred/cited.

I undertake that if I am found guilty of any formal plagiarism in the above titled thesis even after award of M.Phil Degree, the University reserves the right to withdraw/revoke my M.Phil degree and that HEC and the University have the right to publish my name on the HEC/University website on which names of students are placed who submitted plagiarized work.

(Aqsa Shaheen)

Registration No: MMT171022

Acknowledgements

In the name of Allah, the most Gracious and Most Merciful. The precious time leading me toward the completion of my M.Phil was a conspicuous time period of my life which I accomplished with the support of many motivational and inspiring persons. Their existence during my this journey has great significance in order to appreciate the encouragement. I would like to gratefully acknowledge their presence in the results presented here. First of all, I feel obliged to thank my supervisor, **Dr. Muhammad Afzal**. It was a prestigious honor for me to get supervision of such hard working and passionate person full of regularity toward his work and always providing aspiration to his students. The same acknowledgement should also go to **Dr. Muhammad Sagheer**, head of the Mathematics Department (CUST), I deeply appreciate the insight I gained through my association with him. I also feel honored to have such supporting class fellows. Finally, without the backbone and prayers of my family it was impossible to make this thesis in practical existence, so I feel obliged to thank my family for being always with me and bringing all care and support for my career.

(Aqsa Shaheen)

Registration No: MMT171022

Abstract

In this thesis, the two bifurcated cylindrical waveguide problems are discussed by using Mode-Matching technique. First problem deals with the study of a bifurcated cylindrical waveguide bounded by acoustically rigid boundaries along with circular step-discontinuity whilst, in the second problem, one duct is considered to be an elastics shell instead of rigid duct. The scattering energy flux in each duct is calculated and then is plotted numerically by using the truncated form of solution. It is seen that reflection and transmission of energy flux depend upon the bounding conditions of ducts regions as well as on the structural discontinuity.

Contents

List of Figures

Chapter 1

Introduction and Literature Review

1.1 Introduction

In modern era, the noise related problems have gain much attention of researchers and engineers. The major sources of indoor and outdoor noise pollution may occur in heating, ventilation, and air conditioning (HVAC) systems of building, power stations, vehicles etc. The unwanted noise generated by some source propagates through ducts or channels. Thus, to minimize noise the absorbent material and various designs of ducts or channels are used. The present thesis is concerned with mathematical modeling of acoustics propagation in cylindrical duct which contains bifurcation with co-axial cylinder. The bounding properties of guiding structure are assumed to be acoustically rigid or elastics shell. The Mode-Matching technique has been used to find the solution of problems discussed in the thesis.

1.2 Historical Background and Literature Review

Although acoustics waves (also known as sound waves) are nearly as old as the existence of man on earth. The scientific study of acoustics (sound) is generally

considered to have its origin in ancient Greece. During sixth century BC, the Greek philosopher Pythagoras studied how the pitch of the string changed with tension and the tones generated by striking. Galileo established the relationship of pitch of a string to its vibrating length. Joseph Sauveur studied for frequency relation to pitch. Marin Mersenne determined the frequency corresponding to given pitch. Jesuit Priest Athanasius Kircher described that the air was not necessary for the propagation of the sound. Gassendi observed that the speed of sound did not depend on the pitch of the sound, which is contrary to Aristotle view, who had taught that high notes are transmitted faster than low notes. The eighteenth century begin with major development in acoustics as mathematician used the new skills of calculus to explain theories of sound wave advancement. In the nineteenth century the field of mathematical acoustic widened because of Helmholtz in Germany who elaborated the field of physiological acoustic and Lord Rayleigh in England who accumulated and combined the previous knowledge with his own conclusions in acoustic field in his phenomenal work "The Theory of Sound". Also in the nineteenth century Wheatstone, Ohm and Henry formulated the similarity between electricity and acoustics. The twentieth century saw a lot development of technological operations of acoustics bodies. The first application was Sabine's ground breaking in architectural acoustics used for detection of Submarine.

The work presented in this thesis is related the acoustic scattering problems in bifurcated cylindrical waveguides. The study is important with reference to noise reduction problems and has been considered by many authors, for examples see [1–7]. Rawlins [1] considered a cylindrical bifurcation waveguide including absorbent lining at the circular rigid and discussed the scattering of dominant wave mode. He used Weiner-Hopf technique to find the solution of boundary value problem. Nilsson and Brander [8–11] analyzed the propagation of sound in circular duct with and without mean flow in the presence of bulk-reacting lining. Demir and Buyukaksoy [2] studied the radiation of plane mode in cylindrical pipe containing partial impedance loading surfaces. They all used Weiner-Hopf technique to solve the problem. Hassan and Hassan et al [12–14] used Mode-Matching technique to discuss the scattering in trifurcation and pentafurcaion waveguides. In references

[15–24], the Mode-Matching technique to solve the boundary value problems of non-Strum Liouville categories has been discussed. The aim of present study is to apply the Mode-Matching technique to solve the bifurcated cylindrical waveguide problems containing rigid and/or elastic shell type bounding wall conditions. The work on elastic shell can be found in [25–27]. Our work on cylindrical waveguide is organized as fellows:

In chapter-1, introduction, historical background and literature review are discussed.

In chapter-2, some basics definitions related terminologies are given.

In chapter-3, acoustic scattering in a bifurcation cylindrical waveguide containing discontinuity in geometry is discussed.

In chapter-4, the reflection and transmission of acoustic waves in a bifurcation waveguide connected with a shell is analyzed.

Both the boundary value problems of chapter-3 and chapter-4 are solved by using the Mode-Matching technique.

Chapter 2

Preliminaries

2.1 Acoustics

The word acoustics is derived from the Greek word "*akouein*", which means to hear. In 1701, Sauveur was the first who used the term "*acoustics*" for the science of sound. Acoustics was originally the study of small pressure/compression wave that can be identified by human ear. But later in the range of acoustics was extended to infra sound and ultra sound as well. Now a days acoustics has become a branch of physics that deals with the mechanical vibration without restriction on frequency. Acoustic has many branches, for examples structure acoustic, physical acoustic, engineering acoustic, bio acoustic, environmental acoustic, musical acoustic, architectural acoustic etc.

2.2 Acoustics Wave Equation

The propagation of acoustic waves can be discussed in term of differential equation. The derivation of this equation is related to the properties of material medium that can be solid, liquid and gas. Thus, the story goes back to the conservation laws; conservation of mass, conservation of momentum, conservation of energy etc.
Here we derive the wave equation in gas like air. The form of conservation laws is

non-linear in general and thus the wave equation will also be non-linear. But it is very hard to discuss the non-linear form of wave equation. Therefore, the linear approximation theory is used which luckly proved practical too. Here we derive the linear form of wave equation.

2.2.1 Conservation of Mass

The conservation of mass equation is the sum of net mass flowing per unit time to the instantaneous rate of change of mass density

$$\frac{\partial \rho}{\partial t} + \nabla.\,(\rho \mathbf{u}) = 0, \tag{2.1}$$

where $\mathbf{u}$ represents flow velocity and ρ shows instantaneous of mass density.

2.2.2 Conservation of Momentum

The conservation of momentum equation relates the net momentum flowing per volume per unit time to the forces acting on it

$$\frac{\partial \rho \mathbf{u}}{\partial t} = -\nabla.(\rho \mathbf{u})\mathbf{u} - \nabla p + \rho \mathbf{g}, \tag{2.2}$$

where p is pressure, $\mathbf{g}$ the gravitational acceleration, ∇p are exerting forces and $\rho \mathbf{g}$ represent the body forces.
By using equation (2.1), we can write

$$\rho \frac{D\mathbf{u}}{Dt} = -\nabla p + \rho \mathbf{g}, \tag{2.3}$$

where $\dfrac{D}{Dt} = \dfrac{\partial}{\partial t} + \mathbf{u}.\nabla$ is known as the total derivative containing first term to be time derivative and second term is convective term.

2.2.3 Equation of State

The thermodynamic behaviour of compressible fluid can be defined by the equation state. For the perfect gas, the equation of state is

$$p = \rho r T, \tag{2.4}$$

where p is pressure, T stands for temperature, and r gives specific gas constant. For a gas enclosed in a vessel of highly thermally conductive walls, the perfect gas isotherm can be given by

$$\frac{p}{p_0} = \frac{\rho}{\rho_0}, \tag{2.5}$$

where p and p_0 are instantaneous and static pressure, ρ and ρ_0 are instantaneous and static density.

If no heat enter or leaves the system, then the perfect adiabatic condition is given by

$$\frac{p}{p_0} = \left(\frac{\rho}{\rho_0}\right)^{\gamma}, \tag{2.6}$$

where $\gamma = c_p/c_v$ = Ratio of heat capacities.

The compression and rarefaction in a gas can be defined as condensation.i.e

$$s = \frac{\rho - \rho_0}{\rho_0}, \tag{2.7}$$

which yield,

$$\rho = \rho_0(1 + s). \tag{2.8}$$

Using (2.8) into (2.7), we get

$$\frac{p}{p_0} = (1 + s)^{\gamma}. \tag{2.9}$$

Expanding the right hand side of above equation by using Taylor's series

$$\frac{p}{p_0} = 1 + \gamma s + \frac{\gamma(\gamma - 1)}{2!}s^2 + ... \tag{2.10}$$

or

$$\frac{p}{p_0} \approx 1 + \gamma s + O(s^2). \tag{2.11}$$

or

$$\frac{p}{p_0} \approx 1 + \gamma s \quad \text{(linear form)}. \tag{2.12}$$

or

$$p - p_0 = \gamma p_0 s. \tag{2.13}$$

Another approach to find the adiabatic relationship between pressure and density fluctuation is obtained by expanding the pressure p at density ρ_0 using Taylor's series

$$p = p(\rho_0) + \frac{\partial p}{\partial \rho} \mid_{\rho=\rho_0} (\rho - \rho_0) + \frac{\partial^2 p}{\partial \rho^2} \mid_{\rho=\rho_0} (\rho - \rho_0) + ... \tag{2.14}$$

$$p \approx p_0 + \frac{\partial p}{\partial \rho} \mid_{\rho=\rho_0} (\rho - \rho_0). \tag{2.15}$$

or

$$p - p_0 = \frac{\partial p}{\partial \rho} \mid_{\rho=\rho_0} (\rho - \rho_0). \tag{2.16}$$

By comparing (2.13) and (2.16), we have

$$\frac{\partial p}{\partial \rho} \mid_{\rho=\rho_0} (\rho - \rho_0) = \gamma p_0 s. \tag{2.17}$$

Using (2.7) into (2.17), we get

$$\gamma = \frac{\beta}{p_0}, \tag{2.18}$$

where $\beta = \rho_0 \dfrac{\partial p}{\partial \rho} \mid_{\rho=\rho_0}$.
The acoustics pressure at any point defined by

$$P = p - p_0. \tag{2.19}$$

Also from equation (2.16), we define acoustic pressure as

$$P = \beta s. \tag{2.20}$$

2.2.4 Linearized Acoustic Wave Equation

The continuity equation (2.1) can be linearized as

$$\frac{\partial s}{\partial t} + \nabla.\mathbf{u} = 0. \tag{2.21}$$

Here we use the acoustic density $\rho = \rho_0(1 + s)$. The Euler equation of motion of small amplitudes pressure fluctuations is given as:

$$\rho_0 \frac{\partial \mathbf{u}}{\partial t} = -\nabla p. \tag{2.22}$$

Now by taking the divergence of (2.22),

$$\frac{\partial}{\partial t}(\nabla.\mathbf{u}) = -\frac{1}{\rho_0}\nabla^2 p. \tag{2.23}$$

On taking the derivative of (2.21) with respect to t, we have

$$\frac{\partial}{\partial t}(\nabla.\mathbf{u}) = -\frac{\partial^2 s}{\partial t^2}. \tag{2.24}$$

Form (2.23) and (2.24), we can write

$$\frac{\partial^2 s}{\partial t^2} = \frac{1}{\rho_0}\nabla^2 p. \tag{2.25}$$

Using (2.19),

$$\nabla^2 p = \frac{1}{c^2}\frac{\partial^2 p}{\partial t^2}, \tag{2.26}$$

where $c^2 = \beta/\rho_0$. The above equation is known as linearized wave equation.
The wave equation (2.26) can be stated in the form of scalar field potential ψ as,

$$\nabla^2 \psi = \frac{1}{c^2}\frac{\partial^2 \psi}{\partial t^2}. \tag{2.27}$$

2.3 Basic Definitions

The following definitions are taken from [28] and [29].

Waveguide

"A waveguide is a structure that guides waves, such as electromagnetic waves or sound, with minimal loss of energy by restricting expansion to one-dimensional or two. The geometry of a waveguide represents its function. An acoustics waveguide behave like a transmission line in which sound waves propagate."

Amplitude

"The amplitude of vibration denotes the maximum displacement of a vibrating body from its equilibrium position."

Time Period

"The period of oscillation represents the time taken by the vibrating body to complete one cycle of motion. The period of oscillation is also known as the time period and is denoted by T.

$$T = \frac{2\pi}{\omega}$$

where ω is called the circular frequency."

Frequency

"Frequency is defined as the number of times an event occurs per unit of time. It can be denoted by f and can be given as

$$f = \frac{1}{T} \tag{2.28}$$

where T is time period and f is measured in Hertz."

Natural Frequency

"If a system after an initial disturbance is left to vibrate on its own, the frequency with which it oscillates without external forces is known as its natural frequency of vibration."

Decibel Scale

"It is customary to describe sound pressures and intensities using logarithmic scales known as sound levels. One reason for this is the very wide range of sound pressures and intensities encountered in the acoustic environment; audible intensities range from approximately 10^{-12} to $10W/m^2$. Using a logarithmic scale compresses the range of numbers required to describe this wide range of intensities and is also consistent with the fact that humans judge the relative loudness of two sounds by the ratio of their intensities.
The most generally used logarithmic scale for describing sound levels is the decibel (dB) scale. The intensity level IL of a sound of intensity I is defined by

$$IL = 10log(I/I_{ref}) \tag{2.29}$$

where I_{ref} is a reference intensity, IL is expressed in decibels referenced to $I_{ref}(dBreI_{ref})$, and log represents the logarithm to base 10."

Chapter 3

Scattering in a Rigid Bifurcation Cylindrical Waveguide

In this chapter, we discuss the acoustic wave propagation and scattering in a cylindrical ducts. The bounding walls of the ducts are assumed acoustically rigid. The eigen form of propagating modes in duct regions are determined by using separation of variable technique. The eigenfunctions in the respective regions of the ducts are orthogonal in nature and the boundary value problem underlies in Strurm-Liouville category which contains well define orthogonal properties. Thus, the use of Mode-Matching procedure, leads to the accurate solution of the problem. The chapter is organized as follows; The description and mathematical formulation of boundary value problem is given in Section 3.1. Mode-Matching solution is determined in Section 3.2. The derivation for energy/power flux is discussed in Section 3.3. The numerical results of the problem are given in the last Section 3.4.

3.1 Mathematical Formulation

Consider an infinite cylindrical waveguide comprising two semi-infinite duct section of different radii. In dimensional cylindrical co-ordinates $(\bar{r}, \bar{\theta}, \bar{z})$, these radii are $\bar{r} = \bar{b}$ and $\bar{r} = \bar{d}$, for $\bar{d} > \bar{b}$. The left hand region $\bar{z} < \bar{0}$ contains bifurcation with

coaxial cylinder of radius $\bar{r} = \bar{a}$, $\bar{b} > \bar{a}$, where overbar shows that the quantity is dimensionalized. The inside of the duct is filled with compressible fluid of sound speed c and density ρ, whereas outside of the waveguide is in "*vacau*". The geometrical configuration of the waveguide is shown in Figure (3.1).

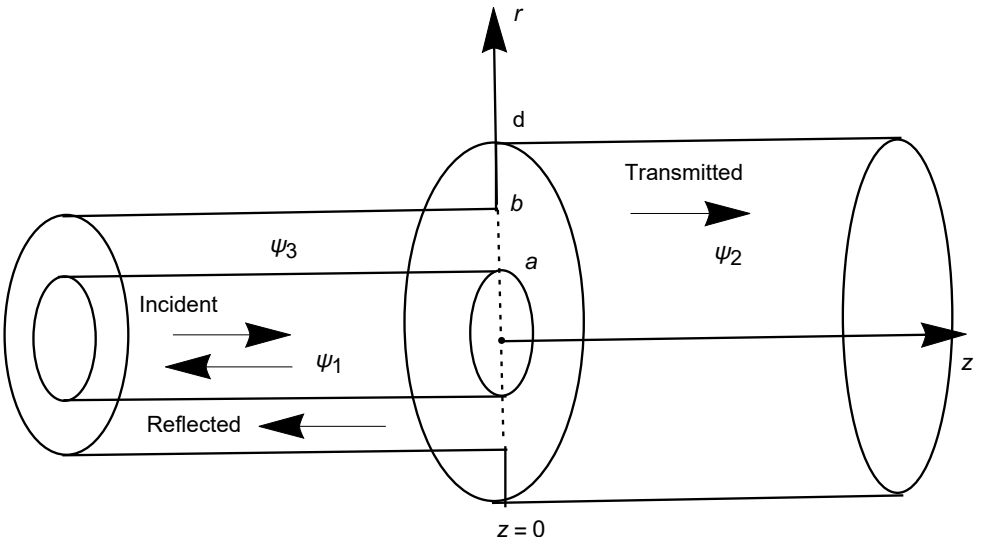

Figure 3.1: Non-dimensional geometry of the waveguide.

Consider an incident wave of harmonic time dependence $e^{-i\omega\bar{t}}$, where $\omega = ck$ is angular velocity, with k being the fluid wavenumber, is propagating from the negative $\bar{z}$-direction towards $\bar{z}$=0. At $\bar{z}$=0, it will scattered into infinite number of modes. Some of modes reflected back in the central and annular region and some of them are transmitted. The acoustics waves propagating inside the duct is governed by the Helmholtz's equation

$$\left\{ \frac{\partial^2}{\partial \bar{r}^2} + \frac{1}{\bar{r}} \frac{\partial}{\partial \bar{r}} + \frac{\partial^2}{\partial \bar{z}^2} + k^2 \right\} \bar{\psi} = 0, \tag{3.1}$$

where $\bar{\psi}$ is the dimensional fluid velocity potential.

The dimensional variables are non-dimensionlize with respect to length scale k^{-1}

and time scale ω^{-1} under transformations:

$$k\bar{r} = r, \quad k\bar{z} = z, \quad k^2\bar{\psi} = \omega\psi. \tag{3.2}$$

Thus, the dimensionless form of (3.1) becomes

$$\left\{ \frac{\partial^2}{\partial r^2} + \frac{1}{r}\frac{\partial}{\partial r} + \frac{\partial^2}{\partial z^2} + 1 \right\} \psi = 0, \tag{3.3}$$

where ψ denotes the dimensionless velocity potential in the duct sections and is given by

$$\psi(r,z) = \begin{cases} \psi_1(r,z) & z < 0, \quad 0 \le r \le a \\ \psi_2(r,z) & z > 0, \quad 0 \le r \le d. \\ \psi_3(r,z) & z < 0, \quad a \le r \le b \end{cases} \tag{3.4}$$

The non-dimensional rigid boundaries are defined as

$$\frac{\partial \psi_1}{\partial r}(a,z) = 0, \quad z < 0, \tag{3.5}$$

$$\frac{\partial \psi_2}{\partial r}(d,z) = 0, \quad z > 0, \tag{3.6}$$

$$\frac{\partial \psi_3}{\partial r}(a,z) = 0, \quad z < 0 \tag{3.7}$$

and

$$\frac{\partial \psi_3}{\partial r}(b,z) = 0, \quad z < 0. \tag{3.8}$$

At interface $z = 0$, the pressure is continuous that is

$$\psi_1(r,0) = \psi_2(r,0), \quad 0 \le r \le a \tag{3.9}$$

and

$$\psi_3(r,0) = \psi_2(r,0), \quad a \le r \le b. \tag{3.10}$$

Also at interface the normal velocities across the region is continuous, that is

$$\frac{\partial \psi_2}{\partial z}(r,0) = \begin{cases} \dfrac{\partial \psi_1}{\partial z}(r,0) & 0 \le r \le a \\ \dfrac{\partial \psi_3}{\partial z}(r,0) & a \le r \le b. \\ 0 & b \le r \le d \end{cases} \tag{3.11}$$

The boundary value problem defined by (3.1)-(3.11) is solved by Mode-Matching technique which is discussed in next section.

3.2 Mode-Matching Solution

In order to find the solution, we consider a fundamental duct mode incident ψ_{inc} from negative z-direction in central cylindrical duct. At $z = 0$, it scatters into infinite reflected and transmitted modes. Thus, the field potential in central region is sum of incident and reflected fields, i.e,

$$\psi_1(r,z) = \psi_{inc} + \psi_{ref},$$

where ψ_{ref} denotes explicitly the superposition of infinite reflected duct modes $\psi_{1n}, n = 0, 1, 2....$ Thus, we may write

$$\psi_1 = \sum_{n=o}^{\infty} A_n \psi_{1n}(r,z),$$

where A_n are the amplitudes of reflected duct modes. The eigen expansion form of transmitted duct is assumed as:

$$\psi_2 = \sum_{n=0}^{\infty} B_n \psi_{2n}(r,z),$$

where B_n are amplitudes and $\psi_{2n}(r,z)$ contains shape of transmitted modes. Similarly, the eigen expansion form of reflected duct modes $\psi_{3n}, n = 0, 1, 2...$ is assumed as

$$\psi_3(r,z) = \sum_{n=0}^{\infty} C_n \psi_{3n}(r,z),$$

where C_n are reflected modes amplitudes. In order to calculate the velocity potential, we use separation of variable method. For this we let

$$\psi_1(r,z) = R_1(r)Z_1(z). \tag{3.12}$$

By substituting (3.12) into (3.3) and then divided by R_1Z_1, we get

$$\frac{R_1''}{R_1} + \frac{1}{r}\frac{R_1'}{R_1} + 1 = -\frac{Z_1''}{Z_1} = \eta^2 \quad \text{(say)}, \tag{3.13}$$

where prime denotes the differentiation with respect to variable involved. From (3.13), we write

$$\frac{R_1''}{R_1} + \frac{1}{r}\frac{R_1'}{R_1} + 1 = \eta^2 \tag{3.14}$$

and

$$-\frac{Z_1''}{Z_1} = \eta^2. \tag{3.15}$$

The solution of (3.15) is

$$Z_1 = c_1 e^{i\eta z} + c_2 e^{-i\eta z},$$

where c_1 and c_2 are arbitrary constants. Note that the exponential terms $e^{-i\eta z}$ and $e^{i\eta z}$ show the propagating mode towards negative and positive z-directions, respectively. To find $R(r)$, we multiplying (3.14) with $r^2R(r)$ to get

$$r^2R_1'' + rR'_1 + r^2(1-\eta^2)R_1 = 0, \tag{3.16}$$

which is Bessel differential equation. The general solution of Bessel equation is

$$R_1(r) = c_3 J_0(\tau r) + c_4 Y_0(\tau r), \tag{3.17}$$

where c_3 and c_4 are arbitrary constants. Here $J_0(\tau r)$ is a Bessel function of first kind and $Y_0(\tau r)$ is of Bessel second kind respectively, where $\tau = (1-\eta^2)^{1/2}$. But as $r \to 0$, the Bessel function of second kind becomes undefined, therefore we must choose $c_4 = 0$ for bounded solution, thus (3.17) becomes

$$R_1(r) = c_3 J_0(\tau r). \tag{3.18}$$

On using (3.18) into (3.5), we get

$$J_0^{'}(\tau a) = 0, \tag{3.19}$$

for non-trivial solution. There are infinite many values of τ for which (3.19) holds. These values are known as the eigenvalues represented by $\tau_n, n = 0, 1, 2, ...$ The corresponding eigenfunctions are

$$R_{1n} = J_0(\tau_n r), \quad n = 0, 1, 2.... \tag{3.20}$$

Hence, the nth mode propagation can be given as

$$\psi_{1n}(r, z) = J_0(\tau_n r) e^{-i\eta_n z}. \tag{3.21}$$

The eigenfunctions defined in (3.20) are orthogonal in nature. To develop orthogonality relation for eigen function τ_n, we rewrite (3.16) and (3.19) as

$$R_{1n}^{''}(r) + \frac{1}{r} R'_{1n}(r) = -\tau_n^2 R_{1n}(r), \tag{3.22}$$

$$R_{1n}^{'}(a) = 0, \tag{3.23}$$

On multiplying (3.23) with $aR_{1m}(a)$, we have

$$aR_{1n}^{'}(a) R_{1m}(a) = 0. \tag{3.24}$$

By interchanging n by m, we found

$$aR_{1m}^{'}(a)R_{1n}(a) = 0. \tag{3.25}$$

On subtracting (3.24) from (3.25), we get

$$a\left[R_{1m}^{'}(a)R_{1n}(a) - R_{1n}^{'}(a)R_{1m}(a)\right] = 0,$$

which yields,

$$\left[r\left\{R_{1m}^{'}(r)R_{1n}(r) - R_{1n}^{'}(r)R_{1m}(r)\right\}\right]_{r=0}^{a} = 0. \tag{3.26}$$

By differentiating it with respect to r, the integral form of (3.26) can be expressed as:

$$\int_0^a \frac{d}{dr}\left[r\left\{R_{1m}^{'}(r)R_{1n}(r) - R_{1n}^{'}(r)R_{1m}(r)\right\}\right]dr = 0,$$

which on simplification leads to,

$$\int_0^a \left[rR_{1n}(r)\left\{R_{1m}^{''}(r) + \frac{1}{r}R_{1m}^{'}(r)\right\} - rR_{1m}(r)\left\{R_{1n}^{''}(r) + \frac{1}{r}R_{1n}^{'}(r)\right\}\right]dr = 0.$$

By using (3.22), we conclude

$$(\tau_n^2 - \tau_m^2)\int_0^a R_{1m}(r)R_{1n}(r)rdr = 0. \tag{3.27}$$

If $(\tau_n^2 - \tau_m^2) \neq 0$, (3.27) leads to

$$\int_0^a R_{1m}(r)R_{1n}(r)rdr = 0. \tag{3.28}$$

If $\tau_n^2 - \tau_m^2 = 0$, $(m = n)$, then integral takes the form

$$\int_0^a R_{1m}(r)R_{1n}(r)rdr = F_n, \tag{3.29}$$

where

$$F_n = \frac{a^2}{2}J_0^2(\tau_n a).$$

On combining (3.28) and (3.29), we found

$$\int_0^a R_{1m}(r)R_{1n}(r)rdr = \delta_{mn}F_n, \tag{3.30}$$

where δ_{mn} is Kronecker delta. Likewise in region $0 \leq r \leq b$, $z > 0$, the separation of variable technique yields the eigenvalues to be roots of the dispersion relation

$$J_0^{'}(\xi_n b) = 0.$$

The corresponding eigenfunctions are

$$R_{2n} = J_0(\xi_n r), \quad n = 0, 1, 2, ...$$

Thus, the propagating nth mode in this region takes the form

$$\psi_{2n} = J_0(\xi_n r)e^{i\lambda_n z},$$

where $\lambda_n = (1 - \xi_n^2)^{1/2}$. Note that, the eigenfunction R_{2n} are orthogonal in nature. The orthogonality relation in this region can be derived in similar fashion as discussed for R_{1n}. Thus the resulting orthogonality relation is found to be

$$\int_0^b R_{2m}(r)R_{2n}(r)rdr = \delta_{mn}D_n \tag{3.31}$$

and

$$D_n = \frac{b^2}{2}J_0^2(\xi_n b).$$

Now we determine the eigenfunctions in annular cylindrical region. In this region the separation of variable technique leads to

$$\psi_{3n} = R_{3n}(r)e^{-is_n z},$$

where $s_n = (1 - \gamma_n^2)^{1/2}$ and

$$R_{3n}(r) = c_5 J_0(\gamma_n r) + c_6 Y_0(\gamma_n r). \tag{3.32}$$

To determine c_5 and c_6 the rigid boundary conditions (3.7) and (3.8) can be written as

$$R_{3n}^{'}(a) = 0, \tag{3.33}$$

$$R_{3n}^{'}(b) = 0. \tag{3.34}$$

By using (3.32) and (3.33), the eigen function R_{3n} takes the form

$$R_{3n}(r) = \frac{c_5}{Y_0^{'}(\gamma_n a)} \left[J_0(\gamma_n r) Y_0^{'}(\gamma_n a) - J_0^{'}(\gamma_n a) Y_0(\gamma_n r) \right], \tag{3.35}$$

where $c_6 = \dfrac{c_5 J_0^{'}(\gamma_n r)}{Y_0^{'}(\gamma_n a)}$.

On using (3.35) into (3.34), we get that γ_n are the roots of following dispersion relation

$$J_0^{'}(\gamma_n b) Y_0^{'}(\gamma_n a) - J_0^{'}(\gamma_n a) Y_0^{'}(\gamma_n b) = 0.$$

Note that the eigenfunctions R_{3n} are orthogonal in nature. To determine their orthogonality relation we rewriting (3.16), (3.33) and (3.34) as

$$R_{3n}^{''}(r) + \frac{1}{r} R^{'}{}_{3n}(r) = -\gamma_n^2 R_{3n}(r), \tag{3.36}$$

$$R_{3n}^{'}(a) = 0, \tag{3.37}$$

$$R_{3n}^{'}(b) = 0, \tag{3.38}$$

where $\gamma_n = (1 - s_n^2)^{1/2}$. On multiplying (3.37) with $aR_{3m}(a)$,

$$aR_{3n}^{'}(a) R_{3m}(a) = 0. \tag{3.39}$$

By interchanging n by m, we found

$$aR_{3m}^{'}(a) R_{3n}(a) = 0. \tag{3.40}$$

By subtracting (3.39) from (3.40), we get

$$a\left[R_{3m}^{'}(a)R_{3n}(a)-R_{3n}^{'}(a)R_{3m}(a)\right]=0. \tag{3.41}$$

On multiplying (3.38) with $bR_{3m}(b)$ it is found that,

$$bR_{3n}^{'}(b)R_{3m}(b)=0, \tag{3.42}$$

which on interchanging n by m, yields

$$bR_{3m}^{'}(b)R_{3n}(b)=0. \tag{3.43}$$

On subtracting (3.42) from (3.43), we found

$$b\left[R_{3m}^{'}(b)R_{3n}(b)-R_{3n}^{'}(b)R_{3m}(b)\right]=0. \tag{3.44}$$

From (3.41) and (3.44), we have

$$b\left[R_{3m}^{'}(b)R_{3n}(b)-R_{3n}^{'}(b)R_{3m}(b)\right]-a\left[R_{3m}^{'}(a)R_{3n}(a)-R_{3n}^{'}(a)R_{3m}(a)\right]=0,$$

which follows

$$\left[r\left\{R_{3m}^{'}(r)R_{3n}(r)-R_{3n}^{'}(r)R_{3m}(r)\right\}\right]_{r=a}^{r=b}=0,$$

or

$$\int_a^b\frac{d}{dr}\left[r\left\{R_{3m}^{'}(r)R_{3n}(r)-R_{3n}^{'}(r)R_{3m}(r)\right\}\right]dr=0. \tag{3.45}$$

The simplification of (3.45) leads to

$$\int_a^b\left[rR_{3n}(r)\left\{R_{3m}^{''}(r)+\frac{1}{r}R_{3m}^{'}(r)\right\}-rR_{3m}(r)\left\{R_{3n}^{''}(r)+\frac{1}{r}R_{3n}^{'}(r)\right\}\right]dr=0.$$

On using (3.36), we get

$$(\gamma_n^2-\gamma_m^2)\int_a^b R_{3m}(r)R_{3n}(r)rdr=0. \tag{3.46}$$

If $\gamma_n^2 - \gamma_m^2 \neq 0$, (3.46) leads to

$$\int_a^b R_{3m}(r)R_{3n}(r)rdr = 0. \tag{3.47}$$

If $\gamma_n^2 - \gamma_m^2 = 0$, $(m = n)$, then integral takes the form

$$\int_a^b R_{3m}(r)R_{3n}(r)rdr = E_n, \tag{3.48}$$

where

$$E_n = \frac{1}{2}\Bigg[b^2\Big\{\Big(J_0^2(b\gamma_n) + J_1^2(b\gamma_n)\Big) - 2J_1(a\gamma_n)Y_1(a\gamma_n)\Big(J_0(b\gamma_n)Y_0(b\gamma_n) + J_1(b\gamma_n)Y_1(b\gamma_n)\Big) + J_1^2(a\gamma_n)\Big(Y_0^2(b\gamma_n) + Y_1^2(b\gamma_n)\Big)\Big\} - \frac{4}{\pi^2\gamma_n}\Bigg].$$

Now combining (3.47) and (3.48), we found

$$\int_a^b R_{3m}(r)R_{3n}(r)rdr = \delta_{mn}E_n. \tag{3.49}$$

where δ_{mn} is Kronecker delta. Now it is convenient to write the eigen expansion form of field potential in three duct regions : that are

$$\psi_1(r,z) = e^{iz} + \sum_{n=0}^{\infty} A_n J_0(\tau_n r)e^{-i\eta_n z}, \tag{3.50}$$

$$\psi_2(r,z) = \sum_{n=0}^{\infty} B_n J_0(\xi_n r)e^{i\lambda_n z}, \tag{3.51}$$

$$\psi_3(r,z) = \sum_{n=0}^{\infty} C_n R_{3n}(r)e^{-is_n z}. \tag{3.52}$$

Note that the first term in (3.50) which is a fundamental duct mode stands for incident field while the second term comprises as reflected field.

In (3.50)-(3.52) the scattering amplitudes $\{A_n, B_n, C_n\}$ are unknowns. These are found by matching conditions. For this we substituted (3.50) and (3.51) into

pressure condition (3.9) to get,

$$1 + \sum_{n=0}^{\infty} A_n J_0(\tau_n r) = \sum_{n=0}^{\infty} B_n J_0(\xi_n r). \tag{3.53}$$

After multiplying the above equation (3.53) with $J_0(\tau_m r)r$ and integrating the resultant, we get

$$\int_0^a J_0(\tau_m r) r dr + \sum_{n=0}^{\infty} A_n \int_0^a J_0(\tau_m r) J_0(\tau_n r) r dr = \sum_{n=0}^{\infty} B_n \int_0^a J_0(\tau_m r) J_0(\xi_n r) r dr. \tag{3.54}$$

On using the orthogonality relation (3.30) in (3.54), it is found that

$$A_m = -\delta_{m0} + \frac{1}{F_m} \sum_{n=0}^{\infty} B_n Q_{mn}, \tag{3.55}$$

where

$$Q_{mn} = \int_o^a J_0(\tau_m r) J_0(\gamma_n r) r dr. \tag{3.56}$$

For $\tau_m \neq \xi_n$, Q_{mn} simplifies to

$$Q_{mn} = \frac{a\left\{\tau_m J_1(\tau_m a) J_0(\xi_n a) - \xi_m J_1(\xi_m a) J_0(\tau_m a)\right\}}{\tau_m^2 - \xi_n^2}.$$

When $\tau_m = \xi_n$, $(m = n)$, it fellows

$$Q_{mm} = \frac{a^2 J_0^2(\tau_m a)}{2}.$$

Similarly on using the scattered fields (3.51) and (3.52) into the normal pressure condition (3.10), we have

$$\sum_{n=0}^{\infty} C_n R_{3n}(r) = \sum_{n=0}^{\infty} B_n J_0(\xi_n r). \tag{3.57}$$

On multiplying (3.57) by $R_{3m}(r)r$ and integrating the resultant with respect to r, $a \leq r \leq b$, we found

$$\sum_{n=0}^{\infty} C_n \int_a^b R_{3m}(r) R_{3n}(r) r dr = \sum_{n=0}^{\infty} B_n \int_a^b R_{3m}(r) J_0(\xi_n r) r dr. \tag{3.58}$$

On using the orthogonality relation (3.49) in (3.58), we get

$$C_m = \frac{1}{E_m}\sum_{n=0}^{\infty} B_n P_{mn}, \tag{3.59}$$

where

$$P_{mn} = \int_a^b R_{3m}(r) J_0(\xi_n r) r dr. \tag{3.60}$$

After simplification, we get

$$P_{mn} = \frac{1}{\xi_n^2 - \gamma_m^2}\Bigg[\xi_n\left\{bJ_1(b\xi_n)\Big(-J_1(a\gamma_m)Y_0(b\gamma_m) + J_0(b\gamma_m)Y_1(a\gamma_m)\Big) + \frac{2J_1(a\xi_n)}{\pi\gamma_m}\right\}$$
$$+ bJ_0(b\xi_n)\gamma_m\Big(-J_1(b\gamma_m)Y_1(a\gamma_m) + J_1(a\gamma_m)Y_1(b\gamma_m)\Big)\Bigg].$$

Finally, we use (3.50), (3.51) and (3.52) in the velocity condition (3.11), to get

$$\sum_{n=0}^{\infty} B_n \lambda_n J_0(\xi_n r) = \begin{cases} 1 - \sum\limits_{n=0}^{\infty} A_n \eta_n J_0(\tau_n r) & 0 \le r \le a \\ -\sum\limits_{n=0}^{\infty} C_n s_n R_{3n} & a \le r \le b. \end{cases} \tag{3.61}$$

By multiplying (3.61) with $J_0(\xi_m r)r$ and integrating the resultant, we get

$$\sum_{n=0}^{\infty} B_n \lambda_n \int_0^d J_0(\xi_n r) J_0(\xi_m r) r dr = \int_0^a J_0(\xi_m r) r dr - \sum_{n=0}^{\infty} A_n \eta_n \int_0^a J_0(\xi_m r) J_0(\tau_n r) r dr$$
$$- \sum_{n=0}^{\infty} C_n s_n \int_a^b J_0(\xi_m r) R_{3n}(r) r dr.$$

By substituting (3.56), (3.60) and the orthogonality relation (3.31), we have

$$B_m = \frac{Q_{m0}}{\lambda_m D_m} - \frac{1}{\lambda_m D_m}\sum_{n=0}^{\infty} A_n \eta_n Q_{nm} - \frac{1}{\lambda_m D_m}\sum_{n=0}^{\infty} C_n s_n P_{nm}, \tag{3.62}$$

where

$$Q_{nm} = \int_0^a J_0(\xi_m r) J_0(\tau_n r) r dr$$

and

$$P_{nm} = \int_a^b J_0(\xi_m r) R_{3n}(r) r dr.$$

In this way the equations (3.55), (3.59) and (3.62) yield a system of equations in which A_m, B_m and C_m are unknowns. These are truncated upto $m = n = 0, 1, 2...N$ terms and solved the equations simultaneously.

3.3 Energy Flux/Power

Here we determine the energy flux in different duct region and then construct the conserved power identity. The non-dimensional form of energy flux can be written as

$$\text{Energy flux} = \text{Re}\left[\int_\Omega i\psi \left(\frac{\partial \psi}{\partial z}\right)^* r dr\right], \tag{3.63}$$

where $(*)$ is the complex conjugate.

To define the incident energy flux, we use incident field $\psi_{inc} = e^{iz}$ into (3.63), we get

$$\text{Incident energy flux} = \text{Re}\left[i\int_0^a e^{iz}(-ie^{-iz})rdr\right],$$
$$\varepsilon^{inc} = \frac{a^2}{2}.$$

Likewise we determinant, the reflection in energy in the central region $0 \leq r \leq a$, we write the reflected field as:

$$\psi_r = \sum_{n=0}^{\infty} A_n J_0(\tau_n r) e^{-i\eta_n z}. \tag{3.64}$$

On using (3.64) and (3.63), we get

Reflected energy flux in region R_1

$$= \text{Re}\left[i\int_0^a \left(\sum_{n=0}^{\infty} A_n J_0(\tau_n r)e^{-i\eta_n z}\right)\left(\sum_{m=0}^{\infty} A_m J_0(\tau_m r)\left(-i\eta_m\right)e^{-i\eta_m z}\right)^* rdr\right],$$

$$= -\text{Re}\left[\sum_{n=0}^{\infty}\sum_{m=0}^{\infty} A_n A_m^* e^{-i(\eta_n - \eta_m^*)}\eta_m^* \int_0^a J_0(\tau_n r)J_0^*(\tau_m r)rdr\right].$$

Note that as τ_n are roots of (3.19) which are real values implies $J_0^*(\tau_m r) = J_0(\tau_m r)$, therefore

$$\text{Reflected energy flux in region } R_1$$
$$= -\text{Re}\left[\sum_{n=0}^{\infty}\sum_{m=0}^{\infty} A_n A_m^* e^{-i(\eta_n - \eta_m^*)}\eta_m^* \int_0^a J_0(\tau_n r)J_0(\tau_m r) r dr\right].$$

On using orthogonality relation (3.30), we get

$$\text{Reflected energy flux in region } R_1 = -\text{Re}\left[\sum_{n=0}^{\infty}\sum_{m=0}^{\infty} A_n A_m^* e^{-i(\eta_n - \eta_m^*)}\eta_m^* F_n \delta_{mn}\right],$$

$$= -\text{Re}\left[\sum_{n=0}^{\infty} \mid A_n \mid^2 \eta_n^* e^{-i(\eta_n - \eta_n^*)} F_n\right].$$

Since $\eta_n = (1-\tau_n)^{1/2}$ is either real or imaginary, thus for real values

$$\text{Reflected energy flux in region } R_1 = -\text{Re}\left[\sum_{n=0}^{\infty} \mid A_n \mid^2 \eta_n F_n\right].$$

Now we determinant, the reflection in energy in region $a \leq r \leq b$, we write the reflected field as:

$$\psi_r = \sum_{n=0}^{\infty} C_n R_{3n}(r) e^{-is_n z}. \tag{3.65}$$

On using (3.65) and (3.63), we get

$$\text{Reflected energy flux in region } R_3$$
$$= \text{Re}\left[i\int_a^b \left(\sum_{n=0}^{\infty} C_n R_{3n}(r) e^{-is_n z}\right)\left(\sum_{m=0}^{\infty} C_m R_{3m}(r)\left(-is_m\right) e^{-is_m z}\right)^* r dr\right],$$

$$= -\text{Re}\left[\sum_{n=0}^{\infty}\sum_{m=0}^{\infty} C_n C_m^* e^{-i(s_n - s_m^*)} s_m^* \int_a^b R_{3n}(r) R_{3m}^*(r) r dr\right].$$

Note that as s_n are roots which are real values implies $R^*_{3m}(r) = R_{3m}(r)$, therefore

$$\text{Reflected energy flux in region } R_3 = -\text{Re}\left[\sum_{n=0}^{\infty}\sum_{m=0}^{\infty} C_n C_m^* e^{-i(s_n - s_m^*)} s_m^* \int_a^b R_{3n}(r) R_{3m}(r) r dr\right].$$

On using orthogonality relation (3.49), we get

$$\text{Reflected energy flux in region } R_3 = -\text{Re}\left[\sum_{n=0}^{\infty}\sum_{m=0}^{\infty} C_n C_m^* e^{-i(s_n - s_m^*)} s_m^* E_n \delta_{mn}\right],$$

$$= -\text{Re}\left[\sum_{n=0}^{\infty} \mid C_n \mid^2 s_n^* e^{-i(s_n - s_n^*)} E_n\right].$$

Since $s_n = (1-\gamma_n)^{1/2}$ is either real or imaginary, thus for real values

$$\text{Reflected energy flux in region } R_3 = -\text{Re}\left[\sum_{n=0}^{\infty} \mid C_n \mid^2 s_n E_n\right].$$

Note that the negative sign on right hand side denotes the energy propagation in negative direction. Similarly for the energy transmission in region $0 \le r \le d$, we write the transmitted field as:

$$\psi_t = \sum_{n=0}^{\infty} B_n J_0(\xi_n r) e^{i\lambda_n z}. \tag{3.66}$$

On using (3.66) and (3.63), we get

$$\text{Reflected energy flux in region } R_2 = \text{Re}\left[i\int_0^d \left(\sum_{n=0}^{\infty} B_n J_0(\xi_n r) e^{i\lambda_n z}\right)\left(\sum_{m=0}^{\infty} B_m J_0(\xi_m r)\,(i\lambda_m)\, e^{i\lambda_m z}\right)^* r dr\right],$$

$$= \text{Re}\left[\sum_{n=0}^{\infty}\sum_{m=0}^{\infty} B_n B_m^* e^{i(\lambda_n - \lambda_m^*)} \lambda_m^* \int_0^d J_0(\xi_n r) J_0^*(\xi_m r) r dr\right].$$

Note that as ξ_n are roots which are real values implies $J_0^*(\xi_m r) = J_0(\xi_m r)$, therefore

$$\text{Reflected energy flux in region } R_2 = \text{Re}\left[\sum_{n=0}^{\infty}\sum_{m=0}^{\infty} B_n B_m^* e^{i(\lambda_n - \lambda_m^*)}\lambda_m^* \int_0^d J_0(\xi_n r) J_0(\xi_m r) r dr\right].$$

On using orthogonality relation (3.31), we get

$$\text{Reflected energy flux in region } R_2 = \text{Re}\left[\sum_{n=0}^{\infty}\sum_{m=0}^{\infty} B_n B_m^* e^{i(\lambda_n - \lambda_m^*)}\lambda_m^* D_n \delta_{mn}\right],$$

$$= \text{Re}\left[\sum_{n=0}^{\infty} \mid B_n \mid^2 \lambda_n^* e^{i(\lambda_n - \lambda_n^*)} D_n\right].$$

Since $\lambda_n = (1 - \xi_n)^{1/2}$ is either real or imaginary, thus for real values

$$\text{Reflected energy flux in region } R_2 = \text{Re}\left[\sum_{n=0}^{\infty} \mid B_n \mid^2 \lambda_n D_n\right].$$

From conversation of energy

$$\text{Left hand energy flux} = \text{Right hand energy flux.}$$

$$\frac{a^2}{2} - \text{Re}\left[\sum_{n=0}^{\infty} \mid A_n \mid^2 \eta_n F_n\right] - \text{Re}\left[\sum_{n=0}^{\infty} \mid C_n \mid^2 s_n E_n\right] = \text{Re}\left[\sum_{n=0}^{\infty} \mid B_n \mid^2 \lambda_n D_n\right]. \tag{3.67}$$

To scale the incident power at unity we multiplying (3.67) by $\frac{2}{a^2}$, after some manipulations we get

$$1 = \mathcal{E}_1 + \mathcal{E}_2 + \mathcal{E}_3, \tag{3.68}$$

which is conserved energy equation, where

$$\mathcal{E}_1 = \frac{2}{a^2}\text{Re}\left[\sum_{n=0}^{\infty} \mid A_n \mid^2 \eta_n F_n\right],$$

$$\mathcal{E}_2 = \frac{2}{a^2}\text{Re}\left[\sum_{n=0}^{\infty} \mid B_n \mid^2 \lambda_n D_n\right]$$

and

$$\mathcal{E}_3 = \frac{2}{a^2}\mathrm{Re}\left[\sum_{n=0}^{\infty} \mid C_n \mid^2 s_n E_n\right].$$

3.4 Numerical Solution

In this section the physical problem is solved numerically after truncation of (3.55) , (3.59) and (3.62) upto $n = 0, 1, 2, ...N$ terms. Here the system is truncated upto N terms. The reduced system contains, $N + 1$ algebraic equations which are solved simultaneously to find the unknown coefficients (A_n, B_n, C_n), $n = 0, 1, 2, ..., N$ terms. The numerical computation are performed in MATHEMATICA using built-in commands. The power distribution in duct regions plotted against the frequency. While carrying the parametric investigation, the physical parameters are chosen as; the speed of sound in air $c = 343ms^{-1}$ density of air $\rho = 1.2043kgm^{-3}$ and the dimensional ducts heights $\bar{a} = 0.3m$, $\bar{b} = 2m$ and $\bar{d} = 2.5m$. We reconstruct our matching conditions at matching interface to validate the truncated solution. The real and imaginary part of non-dimensional pressures and velocities at matching interface are shown in Figures 3.2-3.5. From these figures, It can be seen that the real and imaginary parts of pressures curves across the regions coincide exactly at matching interface as considered in equations (3.9) and (3.10). Likewise in Figures 3.6-3.7 the real and imaginary parts of velocities coincide at apparatus whereas the real and imaginary parts of ψ_{2z} becomes zero when $b \leq r \leq d$. This is exactly that we considered in equation (3.11). In this way the matching conditions confirm the accuracy of performed algebra as well as the truncated solution.

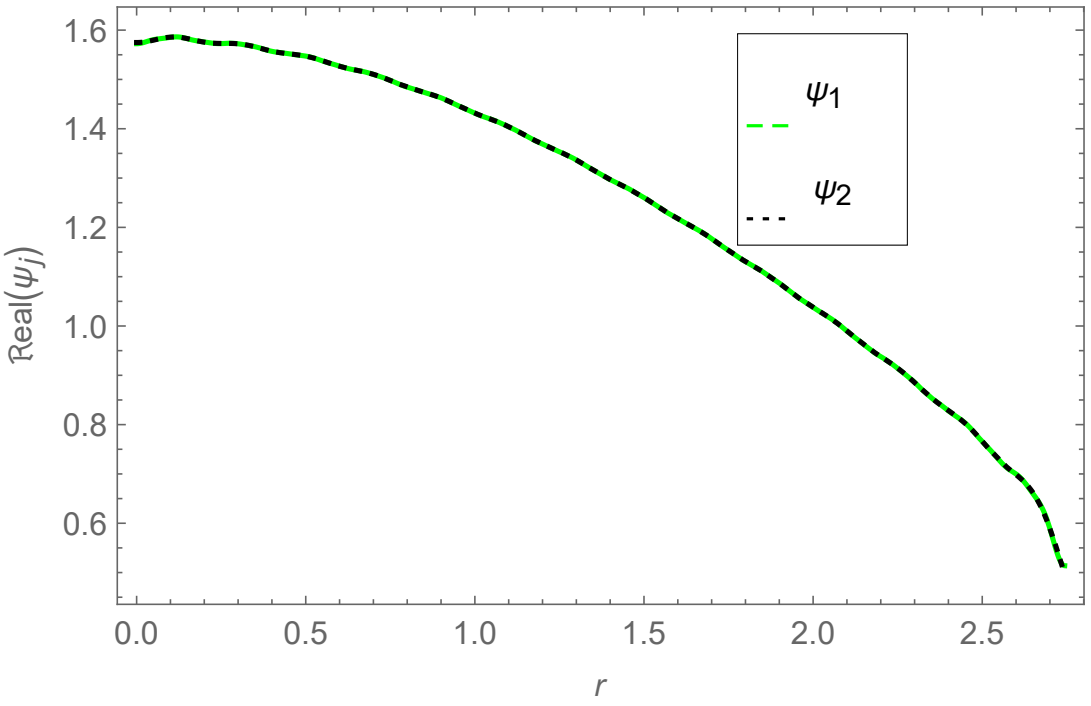

Figure 3.2: Real parts of pressures $\psi_1(r,0)$ and $\psi_2(r,0)$ plotted against r.

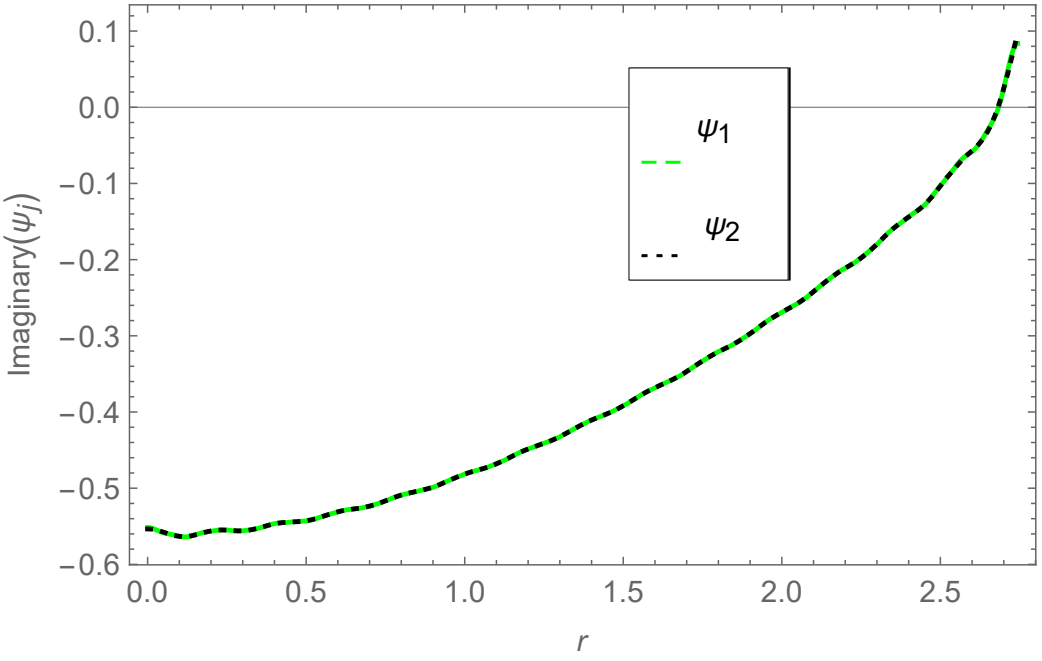

Figure 3.3: Imaginary parts of pressures $\psi_1(r,0)$ and $\psi_2(r,0)$ plotted against r.

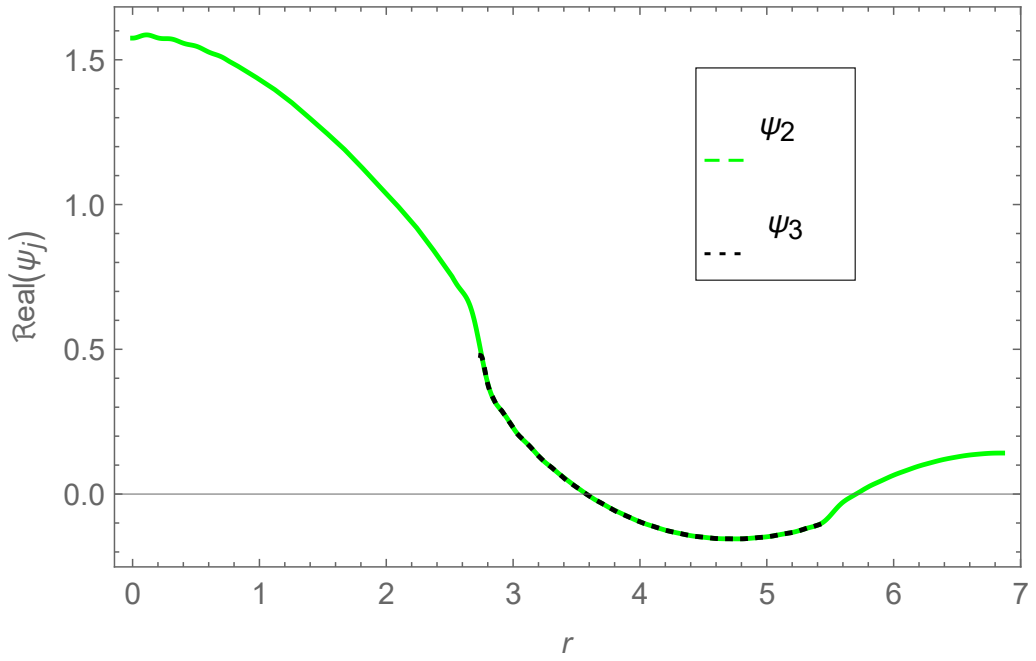

Figure 3.4: Real parts of pressures $\psi_2(r,0)$ and $\psi_3(r,0)$ plotted against r.

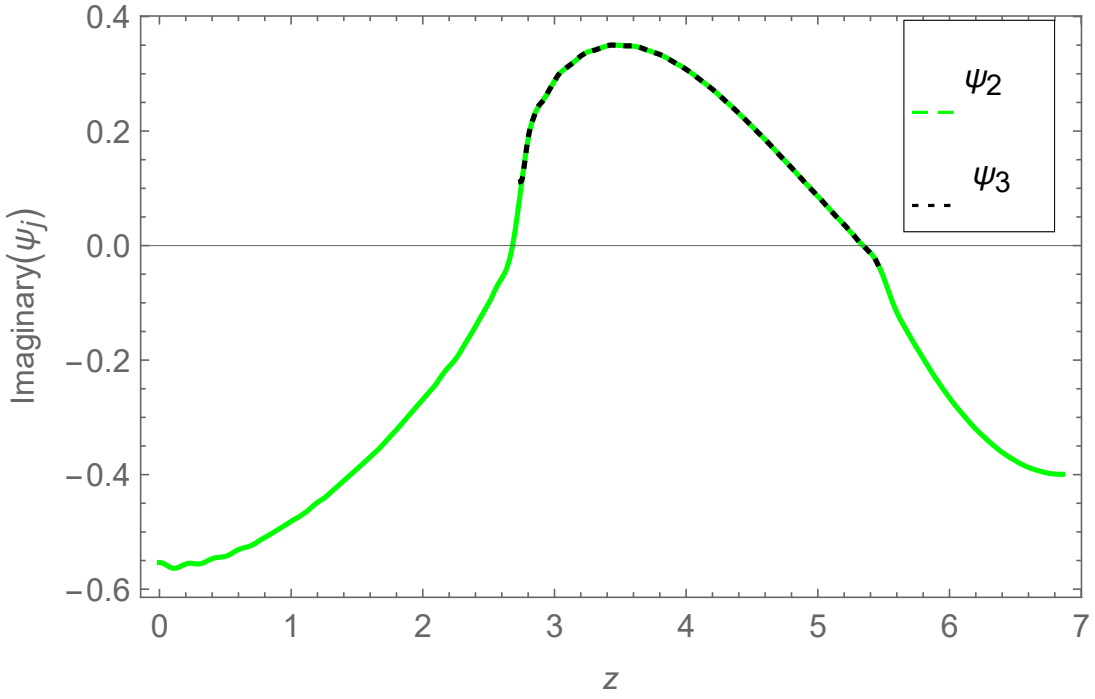

Figure 3.5: Imaginary parts of pressures $\psi_2(r,0)$ and $\psi_3(r,0)$ plotted against r.

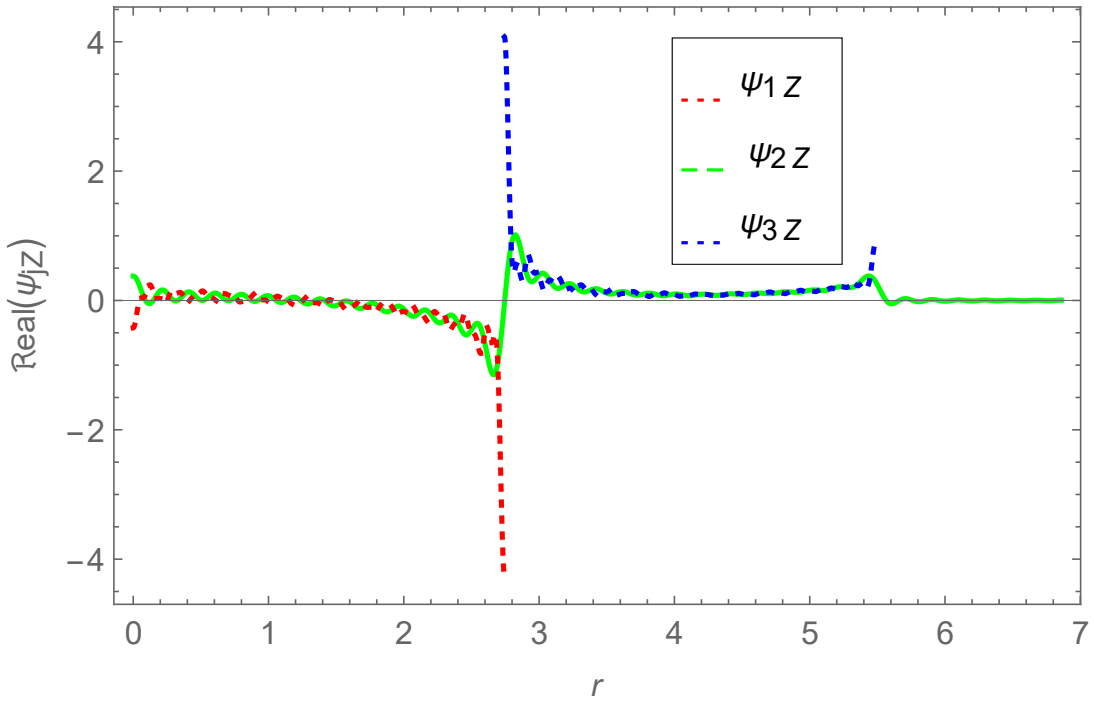

Figure 3.6: Real parts of velocities $\psi_{1z}(r,0)$, $\psi_{2z}(r,0)$ and $\psi_{3z}(r,0)$ plotted against r.

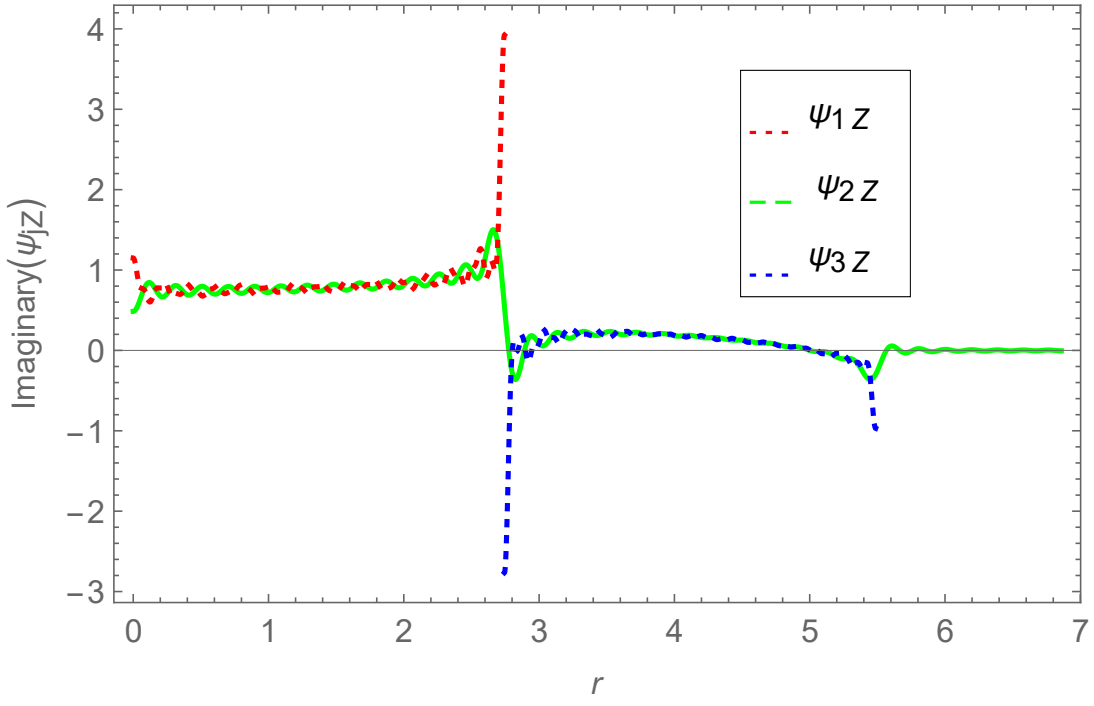

Figure 3.7: Imaginary parts of velocities $\psi_{1z}(r,0)$, $\psi_{2z}(r,0)$ and $\psi_{3z}(r,0)$ plotted against r

Furthermore, the accuracy of truncated solution can be confirmed through energy flux identity. The power components against frequency are plotted in Figures 3.8-3.9 for circular regions of radii $\bar{a} = 0.3m$, $\bar{b} = 2m$ and $\bar{d} = 2.5m$. The roots of involving parameters remain invariant as discussed in the start of this section.
Note that in Figure 3.8 the step-discontinuity is assumed. For the dispersion of energy flux, we plot the reflected and transmitted energy flux against frequency. Moreover, the sum of the scattering power propagation in different regions is unity which justifies the conserved power identity (3.68). In this way the confirmation of matching conditions and conserved power identity validation the truncated solution.
The physical behavior depicted in Figure 3.8, shows that the reflected power in region R_1 increases continuously in frequency regime $1Hz \leq f \leq 276Hz$. After that, it goes on decreasing and start fluctuating to reaches its minimum for higher frequencies. When the reflected power goes on decreasing then the transmitted power goes on increasing. So that, the reflected and transmitted powers are converse to each other.
In Figure 3.9 the step-discontinuity is removed by taking $b = d$, when an fundamental mode becomes propagating then both the reflected and transmitted powers behave smoothly in frequency regime $1Hz \leq f \leq 346Hz$. After that, the reflected power goes on decreasing and at the same time transmitted power goes on increasing fluctuating to reach its minimum and maximum for higher frequencies.
The power components against frequency plotted in Figures 3.10-3.11 for circular regions $\bar{a} = 0.5m$, $\bar{b} = 0.25m$ and $\bar{d} = 3m$. In Figure 3.10 the step-discontinuity is assumed. Furthermore in Figures $3.12-3.13$ the dimensions are fixed as $\bar{a} = 0.8m$, $\bar{b} = 0.3m$ and $\bar{d} = 3.5m$.

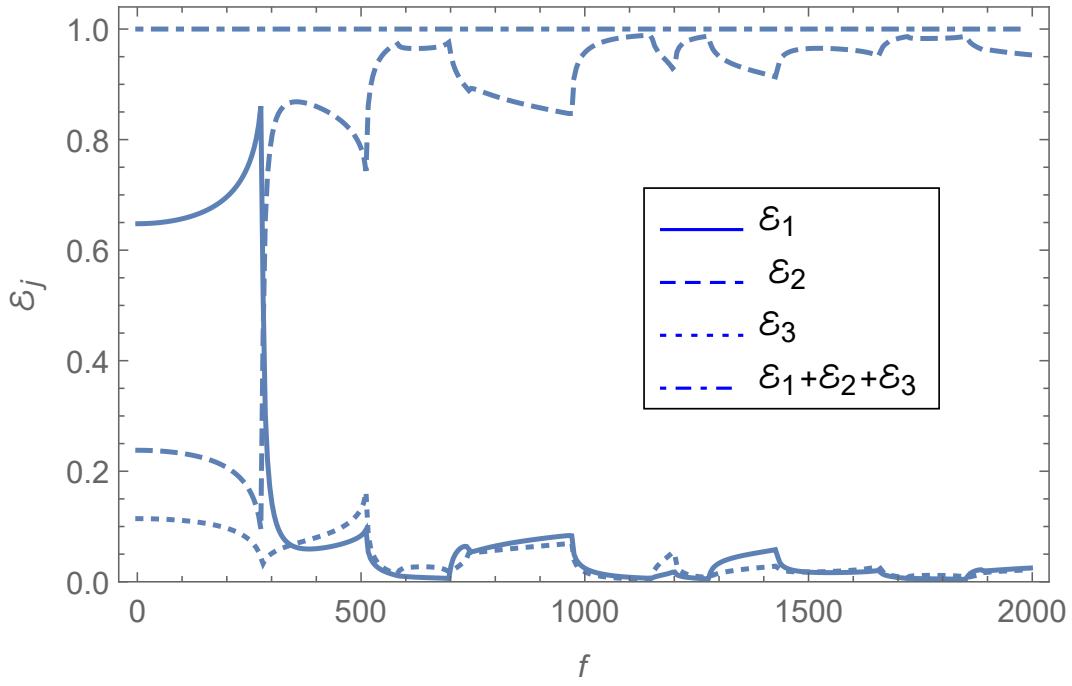

Figure 3.8: Scattered energy flux (ε_j) in regions R_j verses frequency for rigid bounding walls with $\bar{d} > \bar{b}$, where $\bar{a} = 0.3m$, $\bar{b} = 2m$, $\bar{d} = 2.5m$ and $N = 20$.

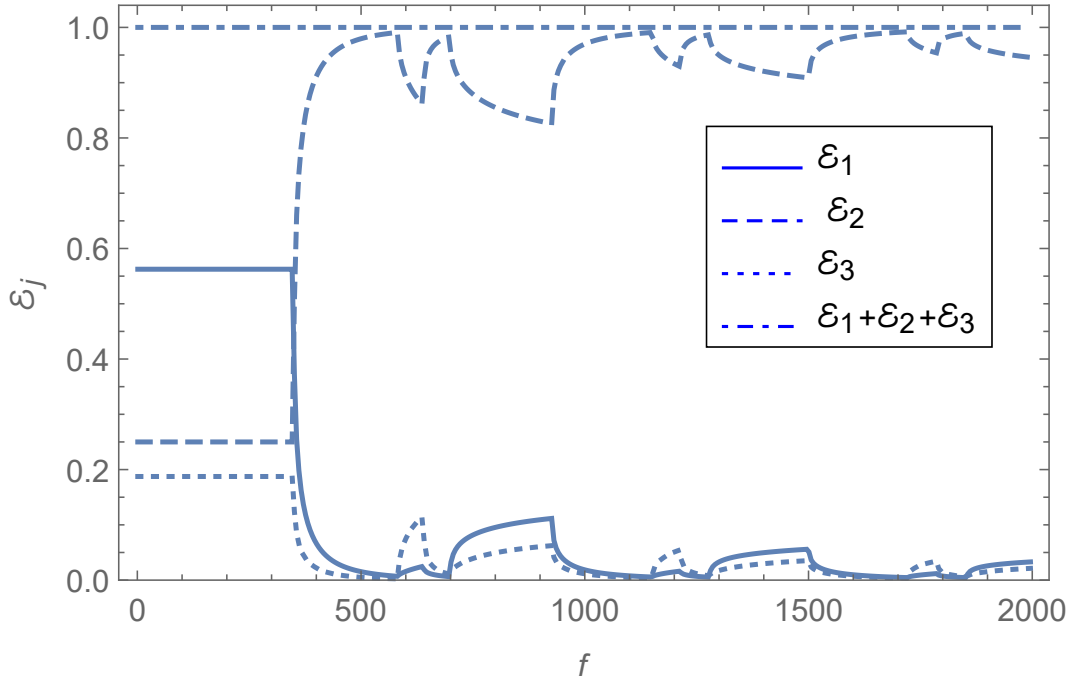

Figure 3.9: Scattered energy in regions $R_j - \varepsilon_j$ verses frequency for rigid bounding walls with $\bar{b} = \bar{d}$, where $\bar{a} = 0.3m$, $\bar{b} = 2m$, $\bar{d} = 2m$ and $N = 20$.

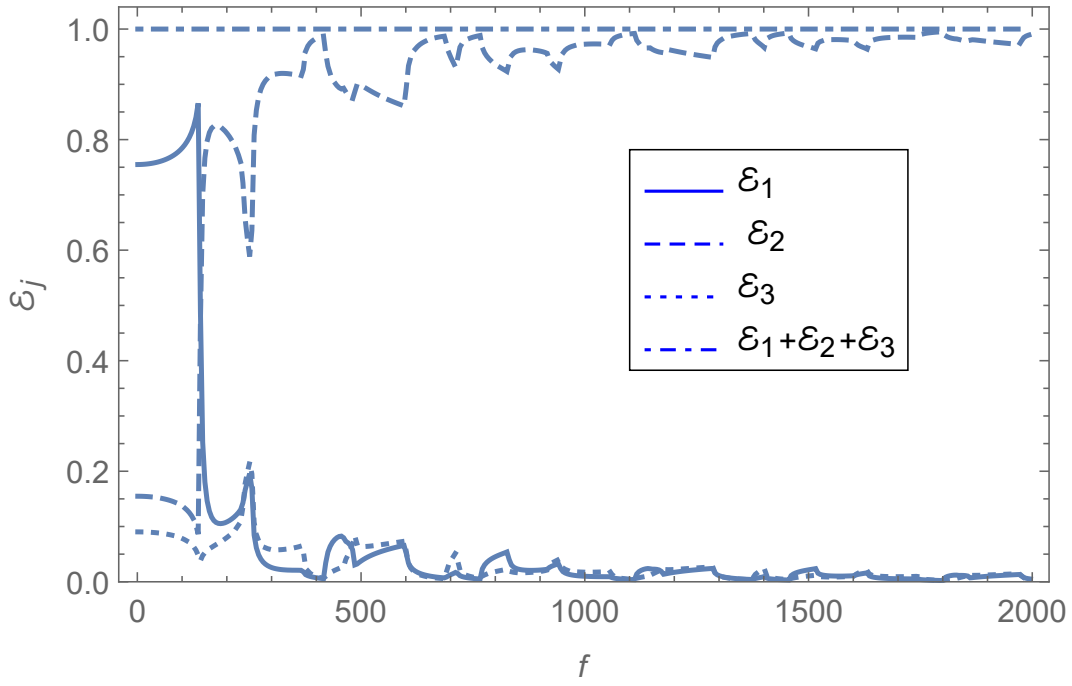

Figure 3.10: Scattered energy flux (ε_j) in regions R_j verses frequency for rigid bounding walls with $\bar{d} > \bar{b}$, where $\bar{a} = 0.5m$, $\bar{b} = 2.5m$, $\bar{d} = 3m$ and $N = 20$.

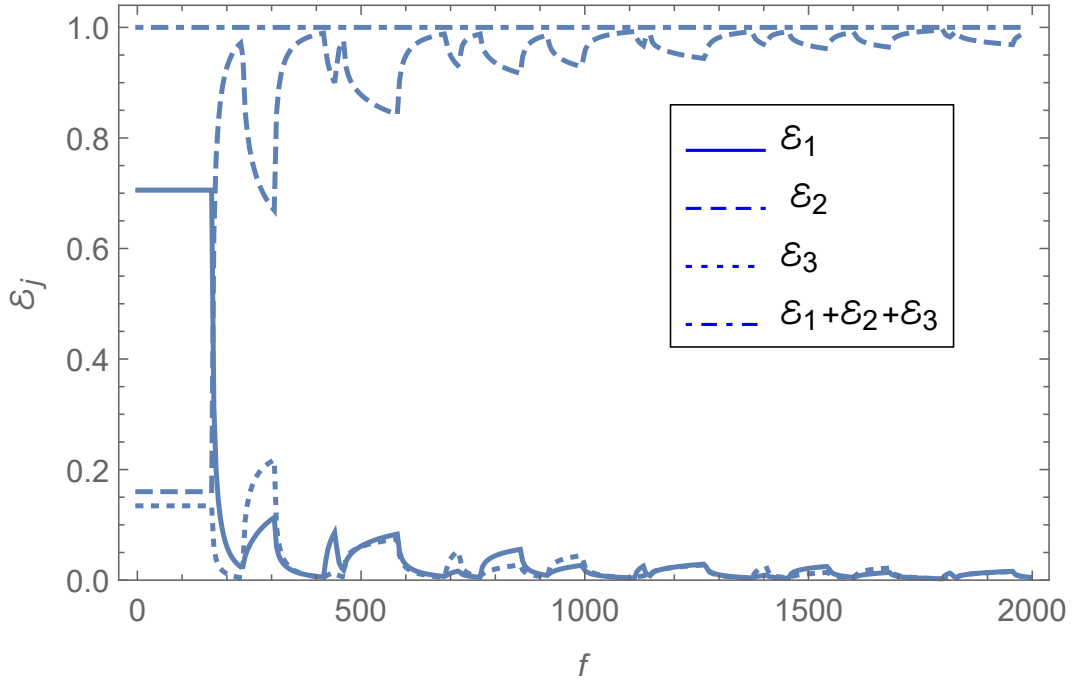

Figure 3.11: Scattered energy in regions $R_j - \varepsilon_j$ verses frequency for rigid bounding walls with $\bar{b} = \bar{d}$, where $\bar{a} = 0.5m$, $\bar{b} = 2.5m$, $\bar{d} = 2.5m$ and $N = 20$.

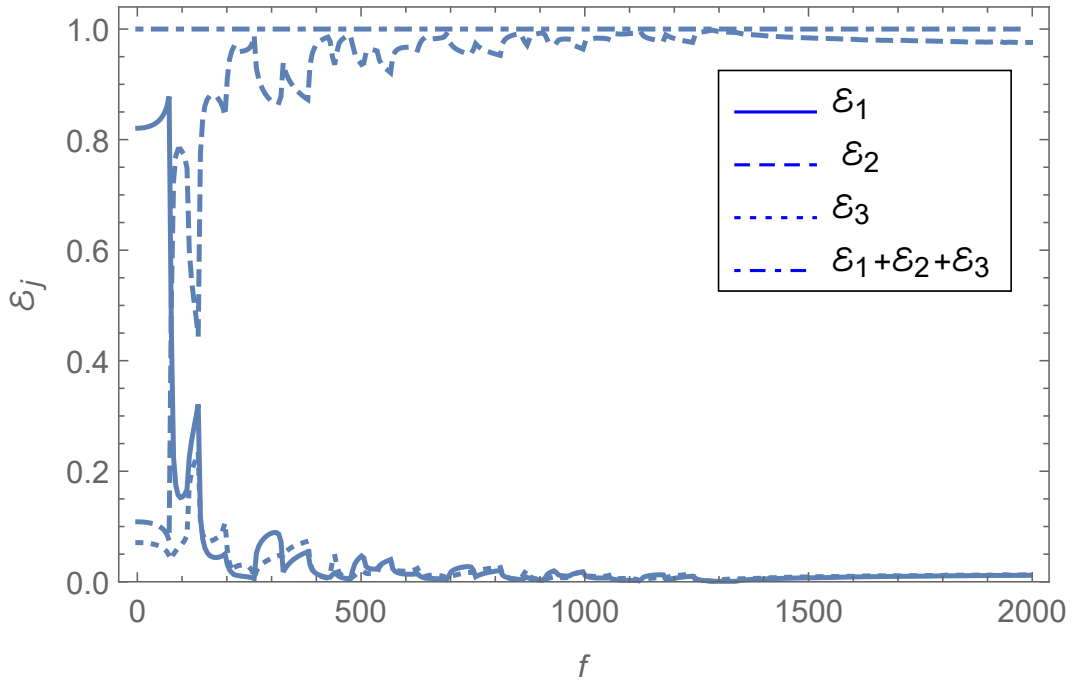

Figure 3.12: Scattered energy in regions $R_j - \varepsilon_j$ verses frequency for rigid bounding walls with $\bar{d} > \bar{b}$, where $\bar{a} = 0.8m$, $\bar{b} = 3m$, $\bar{d} = 3.5m$ and $N = 20$.

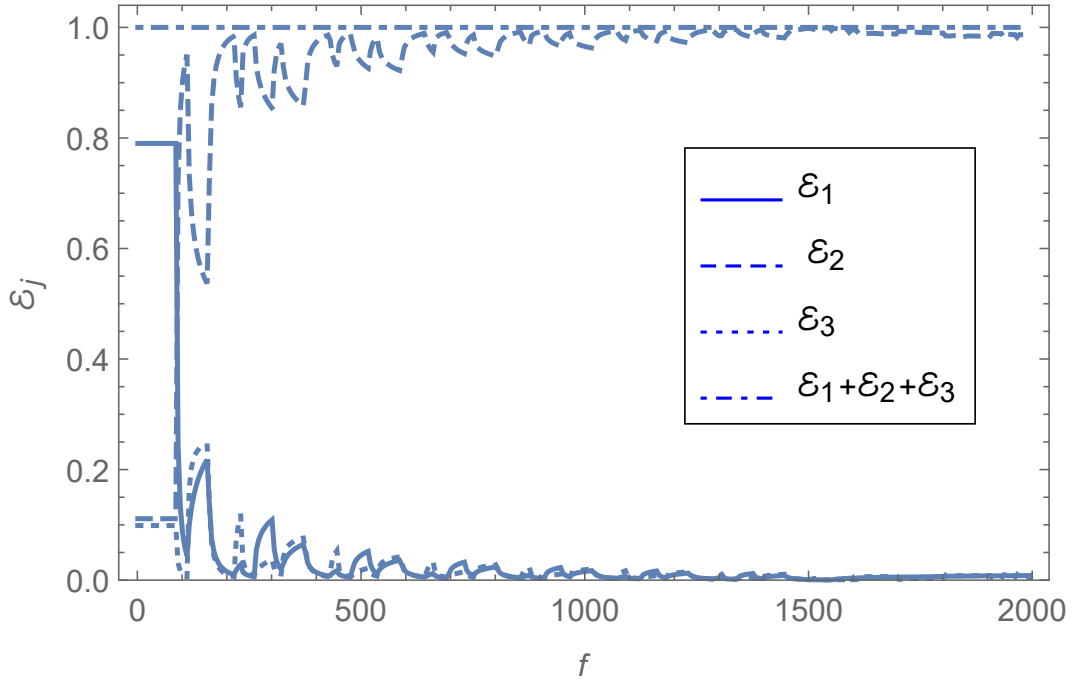

Figure 3.13: Scattered energy in regions $R_j - \varepsilon_j$ verses frequency for rigid bounding walls with $\bar{b} = \bar{d}$, where $\bar{a} = 0.8m$, $\bar{b} = 3m$, $\bar{d} = 3m$ and $N = 20$.

From scattered energy in different regions it can be seen that on increasing the height of step-discontinuity, the reflected power increases whereas transmitted power decreases, while the power balanced is achieved successfully.

Chapter 4

Scattering in Flexible Bifurcated Cylindrical Waveguide

In this chapter, we consider a bifurcated waveguide whose right hand duct is an elastics shell while the rest of the problem remains same as discussed in Chapter-3. The governing equations for left hand regions remain same as given in Chapter-3 whilst for right duct we use Donnell-Mushtari equations of motion as stated by Junger and Feit [25] to describe the dynamics of boundaries. The generalised orthogonality relation developed by Lawrie and Pullen [27] for the elastic shell is used to recaust the differential system into linear algebraic system.
This chapter is arranged as fellows: The mathematical formulation and Mode-Matching solution are given in Sections 4.1 and 4.2, the energy flux/power is discussed in Section 4.3 and the numerical results of the problem is given in Section 4.4.

4.1 Mathematical Formulation

Consider an infinite cylindrical waveguide comprising two semi-infinite duct section of different radii. In dimensional cylindrical co-ordinates $(\bar{r}, \bar{\theta}, \bar{z})$, these radii are $\bar{r} = \bar{b}$ and $\bar{r} = \bar{d}$, for $\bar{d} > \bar{b}$. The left hand region $\bar{z} < \bar{0}$ contains bifurcation

with coaxial cylinder of radius $\bar{r} = \bar{a}$, $\bar{b} > \bar{a}$, where overbar shows the quantity is dimensionalized. The inside of the duct is filled with compressible fluid of sound speed c and density ρ, whereas outside of the waveguide is in "*vacau*". The geometrical configuration of the waveguide is shown in Figure (4.1).

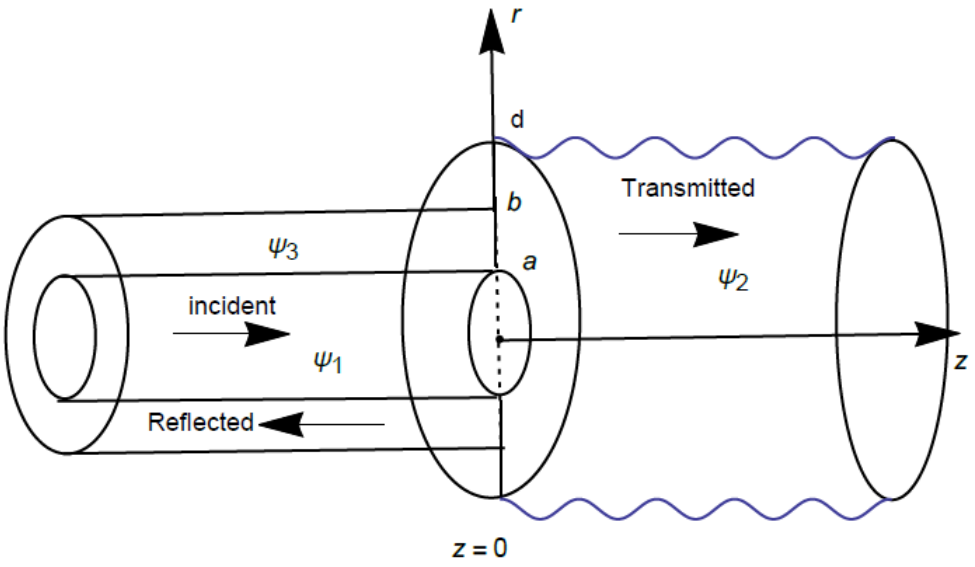

Figure 4.1: Non-dimensional geometry of waveguide.

Considered an incident wave of harmonic time dependence $e^{-i\omega\bar{t}}$, where $\omega = ck$ is annular velocity , with k being the fluid wavenumber, is propagating from the negative $\bar{z}$-direction towards $\bar{z}$=0. At $\bar{z}$=0, it will scattered into infinite number of modes. Some of modes reflected back in the central and annular region and some of them are transmitted. The acoustics waves propagating inside the duct is governed by the Helmholtz's equation

$$\left\{\frac{\partial^2}{\partial\bar{r}^2} + \frac{1}{\bar{r}}\frac{\partial}{\partial\bar{r}} + \frac{\partial^2}{\partial\bar{z}^2} + k^2\right\}\bar{\psi} = 0,$$

where $\bar{\psi}$ is the dimensional field velocity potential.

To describe the motion of a flexible shell, we use the Donnell-Mushtari equations of motion derived by taking the assumption of small displacements as compared to the thickness of shell [27]. "The Donnell-Mushtari equations of motion for a

cylindrical shell of radius $\bar{d}$ are:

$$\frac{\partial^2\bar{u}}{\partial\bar{z}^2}+\frac{1-\nu}{2\bar{d}^2}\frac{\partial^2\bar{u}}{\partial\theta^2}+\frac{1+\nu}{2\bar{d}}\frac{\partial^2\bar{v}}{\partial\bar{z}\partial\theta}+\frac{\nu}{\bar{d}}\frac{\partial\bar{w}}{\partial\bar{z}}+\frac{\omega^2\bar{u}}{c_s^2}=0,\quad \text{at}\quad \bar{r}=\bar{d},$$

$$\frac{1+\nu}{2\bar{d}}\frac{\partial^2\bar{u}}{\partial\bar{z}\partial\theta}+\frac{1-\nu}{2}\frac{\partial^2\bar{v}}{\partial\bar{z}^2}+\frac{1}{\bar{d}^2}\frac{\partial^2\bar{v}}{\partial\theta^2}+\frac{1}{\bar{d}^2}\frac{\partial\bar{w}}{\partial\theta}+\frac{\omega^2\bar{v}}{c_s^2}=0,\quad \text{at}\quad \bar{r}=\bar{d},$$

$$\frac{\nu}{\bar{d}}\frac{\partial\bar{u}}{\partial\bar{z}}+\frac{1}{\bar{d}^2}\frac{\partial\bar{v}}{\partial\theta}+\frac{\bar{w}}{\bar{d}^2}+\frac{h^2}{12}\frac{\partial^4\bar{w}}{\partial\bar{z}^4}+\frac{2h^2}{12\bar{d}^2}\frac{\partial^4\bar{w}}{\partial\bar{z}^2\partial\theta^2}+\frac{h^2}{12\bar{d}^4}\frac{\partial^4\bar{w}}{\partial\theta^4}-\frac{\omega^2\bar{w}}{c_s^2}-\frac{\bar{p}(\bar{d},\bar{z})}{c_s^2\rho_s h}=0,\text{at }\bar{r}=\bar{d}.\text{"}$$

where $\bar{u}$, $\bar{v}$ and $\bar{w}$ are corresponding the longitudinal, circumferential and radial midsurface shell displacements respectively, ν is Poisson's ratio, $\bar{p}(\bar{d},\bar{z})$ is the internal fluid pressure acting on the shell and c_s is the in "*vacuo*" sound speed in the shell given by

$$c_s=\left[\frac{E}{(1-\nu^2)\rho_s}\right]^{1/2},$$

where E is Young's modulus. For axisymmetric motion all θ-dependent displacements can be neglected, which reduces the equations of motion to

$$\frac{\partial^2\bar{u}}{\partial\bar{z}^2}+\frac{\nu}{\bar{d}}\frac{\partial\bar{w}}{\partial\bar{z}}+\frac{\omega^2\bar{u}}{c_s^2}=0,\quad \text{at}\quad \bar{r}=\bar{d},$$

$$\frac{1-\nu}{2}\frac{\partial^2\bar{v}}{\partial\bar{z}^2}+\frac{\omega^2\bar{v}}{c_s^2}=0,\quad \text{at}\quad \bar{r}=\bar{d},$$

$$\frac{\nu}{\bar{d}}\frac{\partial\bar{u}}{\partial\bar{z}}+\frac{\bar{w}}{\bar{d}^2}+\frac{h^2}{12}\frac{\partial^4\bar{w}}{\partial\bar{z}^4}-\frac{\omega^2\bar{w}}{c_s^2}-\frac{\bar{p}(\bar{d},\bar{z})}{c_s^2\rho_s h}=0,\quad \text{at}\quad \bar{r}=\bar{d}.$$

The pressure $\bar{p}$ and the shell displacement $\bar{\omega}$ can be expressed in terms of the velocity potential $\bar{\psi}$ as fellows:

$$\bar{p}=i\omega\rho\bar{\psi}, \tag{4.1}$$

$$\bar{w}=\frac{i}{\omega}\frac{\partial\bar{\psi}}{\partial\bar{r}}. \tag{4.2}$$

On using the above relations given in (4.1) and (4.2), we get

$$\frac{\partial^2\bar{u}}{\partial\bar{z}^2}+\frac{i\nu}{\omega\bar{d}}\frac{\partial^2\bar{\psi}}{\partial\bar{z}\partial\bar{r}}+\frac{\omega^2\bar{u}}{c_s^2}=0,\quad \text{at}\quad \bar{r}=\bar{d}$$

and

$$\frac{\nu}{\bar{d}}\frac{\partial \bar{u}}{\partial \bar{z}} + \frac{i}{\bar{d}^2\omega}\frac{\partial \bar{\psi}}{\partial \bar{r}} + \frac{ih^2}{12\omega}\frac{\partial^5 \bar{\psi}}{\partial \bar{z}^4 \partial \bar{r}} - \frac{i\omega}{c_s^2}\frac{\partial \bar{\psi}}{\partial \bar{r}} - \frac{i\omega\rho\bar{\psi}}{c_s^2\rho_s h} = 0, \quad \text{at} \quad \bar{r} = \bar{d}.$$

The dimensional variables can be non-dimensionalized with respect to typical time scale ω^{-1} and length scale k^{-1} under transformations:

$$k\bar{r} = r, \quad k\bar{z} = z, \quad k^2\bar{\psi} = \omega\psi. \tag{4.3}$$

With the help of above transformation, we define the non-dimensionalized Helmholtz equation as fellow:

$$\left\{\frac{\partial^2}{\partial r^2} + \frac{1}{r}\frac{\partial}{\partial r} + \frac{\partial^2}{\partial z^2} + 1\right\}\psi = 0, \tag{4.4}$$

where ψ is the dimensionaless field velocity potential which can be define in three duct sections as

$$\psi(r,z) = \begin{cases} \psi_1(r,z) & z < 0, \quad 0 \le r \le a \\ \psi_2(r,z) & z > 0, \quad 0 \le r \le d. \\ \psi_3(r,z) & z < 0, \quad a \le r \le b \end{cases}$$

The non-dimensional rigid boundary can be defined as

$$\frac{\partial \psi_1}{\partial r}(a,z) = 0, \quad z < 0.$$

The dimensionaless Donnell-Mushtari equations of motion are as fellows:

$$\frac{\partial^2 u}{\partial z^2} + \frac{i\nu}{d}\frac{\partial^2 \psi_2}{\partial r \partial z} + \beta^2 u = 0, \quad \text{at} \quad r = d, \tag{4.5}$$

$$\frac{1-\nu}{2}\frac{\partial^2 v}{\partial z^2} + \beta^2 v = 0, \quad \text{at} \quad r = d, \tag{4.6}$$

$$-i\nu d\frac{\partial u}{\partial z} + \frac{\partial \psi_2}{\partial r} + \frac{1}{\Gamma}\frac{\partial^5 \psi_2}{\partial r \partial z^4} - d^2\beta^2\frac{\partial \psi_2}{\partial r} - \frac{d^2\beta^2\rho}{\rho_s hk}\psi_2 = 0, \quad \text{at} \quad r = d, \tag{4.7}$$

where $\beta = \omega/(c_s k)$ and $\Gamma = 12/(k^2h^2d^2)$.

Additionally, we improve conditions to define the properties of connections of

shell with rigid ring. It can be clamped or pin-jointed etc. Here only clamped connection is assumed. For a shell that is clamped, the conditions are

$$\bar{u} = \bar{\omega} = \frac{\partial \bar{\omega}}{\partial \bar{z}} = 0, \quad \text{at} \quad \bar{z} = 0 \quad \text{and} \quad \bar{r} = \bar{d}.$$

These edge conditions are non-dimensionalised by using variables given in (4.3),

$$u = \frac{\partial \psi_2}{\partial r} = \frac{\partial^2 \psi_2}{\partial r \partial z} = 0, \quad \text{at} \quad z = 0 \quad \text{and} \quad r = d. \tag{4.8}$$

The rigid boundary condition for velocity potential ψ_2 is defined as

$$\frac{\partial \psi_2}{\partial r}(d, z) = 0, \quad z > 0.$$

For the velocity potential ψ_3 the boundaries conditions are

$$\frac{\partial \psi_3}{\partial r}(a, z) = 0, \quad z < 0,$$

$$\frac{\partial \psi_3}{\partial r}(b, z) = 0, \quad z < 0.$$

At interface $z = 0$, the pressure is continuous that is

$$\psi_1(r, 0) = \psi_2(r, 0), \quad 0 \leq r \leq a, \tag{4.9}$$

$$\psi_3(r, 0) = \psi_2(r, 0), \quad a \leq r \leq b. \tag{4.10}$$

Also at interface the normal velocities across the region is continuous, that is

$$\frac{\partial \psi_2}{\partial z}(r, 0) = \begin{cases} \dfrac{\partial \psi_1}{\partial z}(r, 0) & 0 \leq r \leq a \\ \dfrac{\partial \psi_3}{\partial z}(r, 0) & a \leq r \leq b. \\ 0 & b \leq r \leq d \end{cases} \tag{4.11}$$

The boundary value problem is solved by using the Mode-Matching technique which is discussed in the next section.

4.2 Mode-Matchng Solution

Consider a fundamental duct mode incident from negative z-direction in central cylindrical duct. At $z = 0$, it disperse into infinite modes in which some are reflected and some are transmitted. The formulation of eigen functions and eigen values of scattering modes in left hand regions remain same as discussed in previous Chapter-3, but the eigenfunctions and corresponding eigenvalues are different in right hand duct region. These can be found by using separation of variable method. For this we let

$$\psi_2(r, z) = R_2(r)Z_2(z). \tag{4.12}$$

By substituting (4.12) into (4.4) and then divided by R_2Z_2, we get

$$\frac{R_2''}{R_2} + \frac{1}{r}\frac{R_2'}{R_2} + 1 = -\frac{Z_2''}{Z_2} = \lambda^2 \quad \text{(say)}, \tag{4.13}$$

where prime denotes the differentiation with respect to variable involved. From (4.13), we write

$$\frac{R_2''}{R_2} + \frac{1}{r}\frac{R_2'}{R_2} + 1 = \lambda^2 \tag{4.14}$$

and

$$-\frac{Z_2''}{Z_2} = \lambda^2. \tag{4.15}$$

The solution of (4.15) is

$$Z_2 = c_7 e^{i\lambda z} + c_8 e^{-i\lambda z},$$

where c_7 and c_8 are arbitrary constants. Note that the exponential terms $e^{-i\lambda z}$ and $e^{i\lambda z}$ show the propagating mode towards negative and positive z-directions, respectively. To find $R(r)$, we multiplying (4.14) with $r^2R(r)$ to get

$$r^2R_2'' + rR'_2 + r^2(1 - \lambda^2)R_2 = 0,$$

which is Bessel differential equation having solution

$$R_2(r) = c_9 J_0(\xi r) + c_{10} Y_0(\xi r), \tag{4.16}$$

where c_9 and c_{10} are arbitrary constants. Here $J_0(\xi r)$ and $Y_0(\xi r)$ are Bessel function of first and second kind respectively, where $\xi = (1-\lambda^2)^{1/2}$. But as $r \to 0$, the Bessel function of second kind becomes undefined, therefore we must choose $c_{10} = 0$ for bounded solution, thus (4.16) becomes

$$R_2(r) = c_9 J_0(\xi r).$$

Hence, the n^{th} mode propagation can be given as

$$\psi_{2n}(r, z) = J_0(\xi_n r) e^{i\lambda_n z}. \tag{4.17}$$

On substituting the velocity potential (4.17) into (4.5) and (4.2), the eigen function expansion form of longitudinal and radial displacements are found as

$$u_n(d, z) = \frac{\nu(1-\xi_n^2)^{1/2} \xi_n J_1(\xi_n d) e^{i\lambda_n z}}{[(1-\xi_n^2)^{1/2} - \beta^2] d} \tag{4.18}$$

and

$$w_n(d, z) = \xi_n J_1(\xi_n d) e^{i\lambda_n z}.$$

The longitudinal displacement (4.18) is then used in (4.7) to get the characteristics equation

$$\begin{aligned} K(\xi, d) &= -\Gamma\nu^2(1-\xi^2)\xi J_1(\xi d) + [(1-\xi^2) - \beta^2][(1-\xi^2)^2 - \mu^4]\xi J_1(\xi d) \\ &+ [(1-\xi^2) - \beta^2]\alpha J_0(\xi d) = 0, \end{aligned}$$

where $\mu^4 = \Gamma(d^2\beta^2 - 1)$ and $\alpha = 12\beta^2\rho/(\rho_s h^3 k^3)$.

Thus, the eigen expansion form of field potential in three duct region can be

written as:

$$\psi_1(r,z) = e^{iz} + \sum_{n=0}^{\infty} A_n J_0(\tau_n r) e^{-i\eta_n z}, \quad 0 \le r \le a, \quad z \le 0, \tag{4.19}$$

$$\psi_2(r,z) = \sum_{n=0}^{\infty} B_n J_0(\xi_n r) e^{i\lambda_n z}, \quad 0 \le r \le d, \quad z \ge 0, \tag{4.20}$$

$$\psi_3(r,z) = \sum_{n=0}^{\infty} C_n R_n(r) e^{-is_n z}, \quad a \le r \le b, \quad z \le 0. \tag{4.21}$$

In (4.19) - (4.21) the scattering amplitudes $\{A_n, B_n, C_n\}$ are unknowns which can be determined by using matching conditions of pressure and normal velocities into (4.9) - (4.11). For this, we invoke the potential fields (4.19) and (4.20) into pressure condition (4.9) to get,

$$1 + \sum_{n=0}^{\infty} A_n J_0(\tau_n r) = \sum_{n=0}^{\infty} B_n J_0(\xi_n r). \tag{4.22}$$

After multiplying (4.22) with $J_0(\tau_m r)r$ and integrating the resultant with respect to r, which leads to

$$\int_0^a J_0(\tau_m r) r dr + \sum_{n=0}^{\infty} A_n \int_0^a J_0(\tau_m r) J_0(\tau_n r) r dr = \sum_{n=0}^{\infty} B_n \int_0^a J_0(\tau_m r) J_0(\xi_n r) r dr. \tag{4.23}$$

On using the orthogonality relation which is derived in Chapter-3, i.e,

$$\int_0^a R_m(r) R_n(r) r dr = \delta_{mn} F_n. \tag{4.24}$$

On using (4.24) into (4.23), we find

$$A_m = -\delta_{0m} + \frac{1}{F_m} \sum_{n=0}^{\infty} B_n Q_{mn}, \tag{4.25}$$

where

$$Q_{mn} = \int_0^a J_0(\tau_m r) J_0(\xi_n r) r dr.$$

For $\tau_m \neq \xi_n$, Q_{mn} simplifies to

$$Q_{mn} = \frac{a\{\tau_m J_1(\tau_m a)J_0(\xi_n a) - \xi_m J_1(\xi_m a)J_0(\tau_m a)\}}{\tau_m^2 - \xi_n^2}.$$

When $\tau_m = \xi_n$ $(with \quad m = n)$, it fellows

$$Q_{mm} = \frac{a^2 J_0^2(\tau_m a)}{2}.$$

Similarly on using the scattered fields (4.20) and (4.21) into the pressure condition (4.10), we have

$$\sum_{n=0}^{\infty} C_n R_n(r) = \sum_{n=0}^{\infty} B_n J_0(\xi_n r). \tag{4.26}$$

On multiplying the above equation (4.26) by $R_m(r)r$ and integrating with respect to r, we found

$$\sum_{n=0}^{\infty} C_n \int_a^b R_m(r)R_n(r)rdr = \sum_{n=0}^{\infty} B_n \int_a^b R_m(r)J_0(\xi_n r)rdr.$$

To find the integral on the left-hand side the orthogonality relation which is derived in previous chapter is used,

$$\int_a^b R_m(r)R_n(r)rdr = \delta_{mn}E_m,$$

it is found that,

$$C_m = \frac{1}{E_m}\sum_{n=0}^{\infty} B_n P_{mn}, \tag{4.27}$$

where

$$P_{mn} = \int_a^b R_m(r)J_0(\xi_n r)rdr,$$

which simplification yields,

$$P_{mn} = \frac{1}{\xi_n^2 - \gamma_m^2}\Bigg[\xi_n\Bigg\{bJ_1(b\xi_n)\Big(-J_1(a\gamma_m)Y_0(b\gamma_m) + J_0(b\gamma_m)Y_1(a\gamma_m)\Big) + \frac{2J_1(a\xi_n)}{\pi\gamma_m}\Bigg\}$$
$$+ bJ_0(b\xi_n)\gamma_m\Big(-J_1(b\gamma_m)Y_1(a\gamma_m) + J_1(a\gamma_m)Y_1(b\gamma_m)\Big)\Bigg].$$

Finally, we use (4.19) - (4.21) into (4.11) to get

$$\sum_{n=0}^{\infty} B_n \lambda_n J_0(\xi_n r) = \begin{cases} 1 - \sum\limits_{n=0}^{\infty} A_n \eta_n J_0(\tau_n r) & 0 \le r \le a \\ - \sum\limits_{n=0}^{\infty} C_n s_n R_n(r) & a \le r \le b. \end{cases} \tag{4.28}$$

Multiplying (4.28) by $\frac{\alpha}{d} J_0(\xi_m r) r$ and integrating the resultant from $0 \le r \le d$, we get

$$\sum_{n=0}^{\infty} B_n \lambda_n \frac{\alpha}{d} \int_0^d J_0(\xi_n r) J_0(\xi_m r) r dr = \frac{\alpha}{d} \int_0^a J_0(\xi_m r) r dr -$$
$$\sum_{n=0}^{\infty} A_n \eta_n \frac{\alpha}{d} \int_0^a J_0(\xi_m r) J_0(\tau_n r) r dr - \sum_{n=0}^{\infty} s_n C_n \frac{\alpha}{d} \int_a^b R_n(r) J_0(\xi_m r) r dr. \tag{4.29}$$

The orthogonality relation as derived by Lawrie Pullen [27] is

$$\frac{\alpha}{d} \int_0^d J_0(\xi_n r) J_0(\xi_m r) r dr = \delta_{mn} D_n - \Bigg[\frac{\Gamma \nu^2 \beta^2}{(\lambda_n^2 - \beta^2)(\lambda_m^2 - \beta^2)} + 2$$
$$- \xi_m^2 - \xi_n^2 \Bigg] \xi_n J_1(\xi_n d) \xi_m J_1(\xi_m d), \tag{4.30}$$

where $\Gamma = \dfrac{12}{h^2 k^2 d^2}$, ξ_n are equivalent wavenumbers, and $\xi_n = (1 - \delta^2)^{1/2}$.
On using (4.30) into (4.29), after some rearrangements, we obtain

$$B_m = \frac{\xi_m J_1(\xi_m d)}{\lambda_m D_m (\lambda_m^2 - \beta^2)} E_0 + \frac{(2 - \xi_m^2) \xi_m J_1(\xi_m d)}{\lambda_m D_m} E1 - \frac{\xi_m J_1(\xi_m d)}{\lambda_m D_m} E_2$$
$$+ \frac{\alpha}{d \lambda_m D_m} Q_{0m} - \frac{\alpha}{d \lambda_m D_m} \sum_{n=0}^{\infty} A_n \eta_n Q_{nm} - \frac{\alpha}{d \lambda_m D_m} \sum_{n=0}^{\infty} C_n s_n P_{nm},$$

where

$$E_0 = \Gamma \nu^2 \beta^2 \sum_{n=0}^{\infty} \frac{B_n \lambda_n \xi_n J_1(\xi_n d)}{(\lambda_n^2 - \beta^2)}, \tag{4.31}$$

$$E_1 = \sum_{n=0}^{\infty} B_n \lambda_n \xi_n J_1(\xi_n d), \tag{4.32}$$

$$E_2 = \sum_{n=0}^{\infty} B_n \lambda_n \xi_n^3 J_1(\xi_n d),$$

are constants and

$$Q_{nm} = \int_0^a J_0(\xi_m r) J_0(\tau_m r) r dr$$

and

$$P_{nm} = \int_a^b R_n(r) J_0(\xi_m r) r dr.$$

To determine the values of constants $E_0 - E_2$, we use edge conditions. For clamped connections we invoke the displacement (4.18) and (4.20) into (4.8) to get

$$\sum_{m=0}^{\infty} \frac{B_m \lambda_m \xi_m J_1(\xi_m d)}{(\lambda_m^2 - \beta^2)} = 0, \tag{4.33}$$

$$\sum_{m=0}^{\infty} B_m \xi_m J_1(\xi_m d) = 0, \tag{4.34}$$

$$\sum_{m=0}^{\infty} B_m \lambda_m \xi_m J_1(\xi_m d) = 0. \tag{4.35}$$

By comparing (4.31) and (4.32) with (4.33) and (4.35), we found $E_0 = E_1 = 0$.

$$B_m = -\frac{\xi_m J_1(\xi_m d)}{\lambda_m D_m} E_2 + \frac{\alpha}{d\lambda_m D_m} Q_{0m} - \frac{\alpha}{d\lambda_m D_m} \sum_{n=0}^{\infty} A_n \eta_n Q_{nm} - \frac{\alpha}{d\lambda_m D_m} \sum_{n=0}^{\infty} C_n s_n P_{nm}. \tag{4.36}$$

To calculate E_2, we multiply (4.36) with $\xi_m J_1(\xi_m d)$ then taking summation over m from 0 to ∞, we obtain Multiplying the above equation by and summing over , we get

$$\sum_{m=0}^{\infty} B_m \xi_m J_1(\xi_m d) = -\sum_{m=0}^{\infty} \frac{\xi_m^2 J_1^2(\xi_m d)}{\lambda_m D_m} E_2 + \frac{\alpha}{d\lambda_m D_m} \sum_{m=0}^{\infty} \xi_m J_1(\xi_m d) \left[Q_{0m} - \sum_{n=0}^{\infty} A_n \eta_n Q_{nm} - \sum_{n=0}^{\infty} C_n s_n P_{nm} \right].$$

On using (4.34), after simplification we get the expression for E_2

$$E_2 = \frac{\alpha}{d\lambda_m D_m S} \sum_{m=0}^{\infty} \xi_m J_1(\xi_m d) \left\{ Q_{0m} - \sum_{n=0}^{\infty} A_n \eta_n Q_{nm} - \sum_{n=0}^{\infty} C_n s_n P_{nm} \right\},$$

where

$$S = \sum_{m=0}^{\infty} \frac{\xi_m^2 J_1^2(\xi_m d)}{\lambda_m D_m}.$$

In this way the equations (425), (4.27) and (4.36) yield a system of equations in which A_m, B_m and C_m are unknowns. These are truncated upto $m = n = 0, 1, 2...N$ terms and solved the equations simultaneously.

4.3 Energy Flux/Power

Here we determine the energy flux in different duct regions and then construct the conserved power identity. To define the incident energy flux, we use incident field $\psi_{inc} = e^{iz}$ into (3.63) which is discussed in chapter-3, we get

$$\text{Incident energy flux} = \text{Re}\left[i\int_0^a e^{iz}(-ie^{-iz})rdr\right],$$
$$\varepsilon^{inc} = \frac{a^2}{2}.$$

Now we determinant, the reflection in energy in the central region $0 \leq r \leq a$, we write the reflected field as:

$$\psi_r = \sum_{n=0}^{\infty} A_n J_0(\tau_n r) e^{-i\eta_n z}. \tag{4.37}$$

By substituting (4.37) into energy flux equation (3.63), we get

Reflected energy flux in region R_1

$$= \text{Re}\left[i\int_0^a \left(\sum_{n=0}^{\infty} A_n J_0(\tau_n r)e^{-i\eta_n z}\right)\left(\sum_{m=0}^{\infty} A_m J_0(\tau_m r)\left(-i\eta_m\right)e^{-i\eta_m z}\right)^* rdr\right],$$

$$= -\text{Re}\left[\sum_{n=0}^{\infty}\sum_{m=0}^{\infty} A_n A_m^* e^{-i(\eta_n - \eta_m^*)}\eta_m^* \int_0^a J_0(\tau_n r)J_0^*(\tau_m r)rdr\right].$$

Note that as τ_n are roots of (3.19) which are real values implies $J_0^*(\tau_m r) = J_0(\tau_m r)$, therefore

$$\text{Reflected energy flux in region } R_1$$
$$= -\text{Re}\left[\sum_{n=0}^{\infty}\sum_{m=0}^{\infty} A_n A_m^* e^{-i(\eta_n - \eta_m^*)}\eta_m^* \int_0^a J_0(\tau_n r) J_0(\tau_m r) r dr\right].$$

On using orthogonality relation (3.30), we get

$$\text{Reflected energy flux in region } R_1 = -\text{Re}\left[\sum_{n=0}^{\infty}\sum_{m=0}^{\infty} A_n A_m^* e^{-i(\eta_n - \eta_m^*)}\eta_m^* F_n \delta_{mn}\right],$$

$$= -\text{Re}\left[\sum_{n=0}^{\infty} \mid A_n \mid^2 \eta_n^* e^{-i(\eta_n - \eta_n^*)} F_n\right].$$

Since $\eta_n = (1-\tau_n)^{1/2}$ is either real or imaginary, thus for real values

$$\text{Reflected energy flux in region } R_1 = -\text{Re}\left[\sum_{n=0}^{\infty} \mid A_n \mid^2 \eta_n F_n\right].$$

Now we determinant, the reflection in energy in region $a \leq r \leq b$, we write the reflected field as:

$$\psi_r = \sum_{n=0}^{\infty} C_n R_{3n}(r) e^{-is_n z}. \tag{4.38}$$

On using (4.38) and (3.63), we get

$$\text{Reflected energy flux in region } R_3$$
$$= \text{Re}\left[i\int_a^b \left(\sum_{n=0}^{\infty} C_n R_{3n}(r) e^{-is_n z}\right)\left(\sum_{m=0}^{\infty} C_m R_{3m}(r)\left(-is_m\right) e^{-is_m z}\right)^* r dr\right],$$

$$= -\text{Re}\left[\sum_{n=0}^{\infty}\sum_{m=0}^{\infty} C_n C_m^* e^{-i(s_n - s_m^*)} s_m^* \int_a^b R_{3n}(r) R_{3m}^*(r) r dr\right].$$

Note that as s_n are roots which are real values implies $R^*_{3m}(r) = R_{3m}(r)$, therefore

$$\text{Reflected energy flux in region } R_3$$
$$= -\text{Re}\left[\sum_{n=0}^{\infty}\sum_{m=0}^{\infty} C_n C_m^* e^{-i(s_n - s_m^*)} s_m^* \int_a^b R_{3n}(r) R_{3m}(r) r dr\right].$$

On using orthogonality relation (3.49), we get

$$\text{Reflected energy flux in region } R_3 = -\text{Re}\left[\sum_{n=0}^{\infty}\sum_{m=0}^{\infty} C_n C_m^* e^{-i(s_n - s_m^*)} s_m^* E_n \delta_{mn}\right],$$

$$= -\text{Re}\left[\sum_{n=0}^{\infty} \mid C_n \mid^2 s_n^* e^{-i(s_n - s_n^*)} E_n\right].$$

Since $s_n = (1 - \gamma_n)^{1/2}$ is either real or imaginary, thus for real values

$$\text{Reflected energy flux in region } R_3 = -\text{Re}\left[\sum_{n=0}^{\infty} \mid C_n \mid^2 s_n E_n\right].$$

Now we calculate the energy flux for region R_2. For this we have the transmitted field given by

$$\psi_{tr} = \sum_{n=0}^{\infty} B_n J_0(\xi_n r) e^{i\lambda_n z}. \tag{4.39}$$

By substituting (4.39) into energy flux equation (3.63), we get

$$\text{Transmitted energy flux in region } R_2$$
$$= \text{Re}\left[i\int_0^b \left(\sum_{n=0}^{\infty} B_n J_0(\xi_n r) e^{i\lambda_n z}\right)\left(\sum_{m=0}^{\infty} B_m J_0(\xi_m r)\,(i\lambda_m)\, e^{i\lambda_m z}\right)^* r dr\right],$$

$$= \text{Re}\left[\sum_{n=0}^{\infty}\sum_{m=0}^{\infty} B_n B_m^* e^{i(\lambda_n - \lambda_m^*)} \lambda_m^* \int_0^b J_0(\xi_n r) J_0^*(\xi_m r) r dr\right].$$

Note that as ξ_n are roots of (4.17) which are real values implies $J_0^*(\xi_m r) = J_0(\xi_m r)$, therefore

$$= \text{Re}\left[\sum_{n=0}^{\infty}\sum_{m=0}^{\infty} B_n B_m^* e^{i(\lambda_n - \lambda_m^*)} \lambda_m^* \int_0^b J_0(\xi_n r) J_0(\xi_m r) r dr\right].$$

On using orthogonality relation (4.30), we get

$$\text{Tranmitted energy flux in region } R_2 = \frac{d}{\alpha}\text{Re}\left[\sum_{n=0}^{\infty}\sum_{m=0}^{\infty} B_n B_m^* e^{i(\lambda_n-\lambda_m^*)}\lambda_m^* D_n \delta_{mn}\right],$$

$$= \frac{d}{\alpha}\text{Re}\left[\sum_{n=0}^{\infty} \mid B_n \mid^2 \lambda_n^* e^{i(\lambda_n-\lambda_n^*)} D_n\right].$$

Since $\lambda_n = (1-\xi_n)^{1/2}$ is either real or imaginary, thus for real values

$$\text{Transmitted energy flux in region } R_2 = \frac{d}{\alpha}\text{Re}\left[\sum_{n=0}^{\infty} \mid B_n \mid^2 \lambda_n D_n\right].$$

From conversation of energy

$$\text{Left hand energy flux} = \text{Right hand energy flux.}$$

$$\frac{a^2}{2} - \text{Re}\left[\sum_{n=0}^{\infty} \mid A_n \mid^2 \eta_n F_n\right] - \text{Re}\left[\sum_{n=0}^{\infty} \mid C_n \mid^2 s_n E_n\right] = \frac{d}{\alpha}\text{Re}\left[\sum_{n=0}^{\infty} \mid B_n \mid^2 \lambda_n D_n\right]. \tag{4.40}$$

To scale the incident power at unity we multiplying (4.40) by $\frac{2}{a^2}$, after some manipulations we get

$$1 = \mathcal{E}_1 + \mathcal{E}_2 + \mathcal{E}_3, \tag{4.41}$$

which is conserved energy equation, where

$$\mathcal{E}_1 = \frac{2}{a^2}\text{Re}\left[\sum_{n=0}^{\infty} \mid A_n \mid^2 \eta_n F_n\right],$$

$$\mathcal{E}_2 = \frac{2d}{a^2\alpha}\text{Re}\left[\sum_{n=0}^{\infty} \mid B_n \mid^2 \lambda_n D_n\right]$$

and

$$\mathcal{E}_3 = \frac{2}{a^2}\text{Re}\left[\sum_{n=0}^{\infty} \mid C_n \mid^2 s_n E_n\right].$$

4.4 Numerical Solution

In this section the physical problem is solved numerically after truncation of (4.25) , (4.27) and (4.36) upto $n = 0, 1, 2, ...N$ terms. Here the system is truncated upto N terms. The reduced system contains, $N + 1$ algebraic equations which are solved simultaneously to find the unknown coefficients (A_n, B_n, C_n), $n = 0, 1, 2, ..., N$ terms. The numerical computation are performed in MATHEMATICA using built-in commands. The power distribution in duct regions is plotted against the frequency.

While carrying the parametric investigation, the physical parameters are chosen as; the speed of sound in air $c = 343ms^{-1}$, density of air $\rho = 1.2043kgm^{-3}$ and the dimensional ducts height are $\bar{a} = 0.1$, $\bar{b} = 0.15$ and $\bar{d} = 0.2$. In addition, an aluminium shell of thickness $h = 0.002$m and of density $\rho_s = 2700\text{kgm}^{-3}$ is consider. The value of poisson's ratio and Young's modulus are taken to be $\nu = 0.34$ and $\text{E} = 7.2 \times 10^{10}\text{Nm}^{-2}$.

We reconstruct our matching conditions at matching interface to validate the truncated solution. The real and imaginary part of non-dimensional pressures and velocities at matching interface are shown in Figure 4.2-4.5.

From these figures, it can be seen that the pressure curves match exactly at matching interface as considered in equation (4.9) and (4.10).

Likewise in Figure 4.6-4.7 the real and imaginary parts of velocities coincide at apparatus whereas the real and imaginary parts of ψ_2 becomes zero when $b \leq r \leq d$. This is exactly that we considered in equation (4.11). In this way the matching conditions confirm the accuracy of performed algebra as well as the truncated solution.

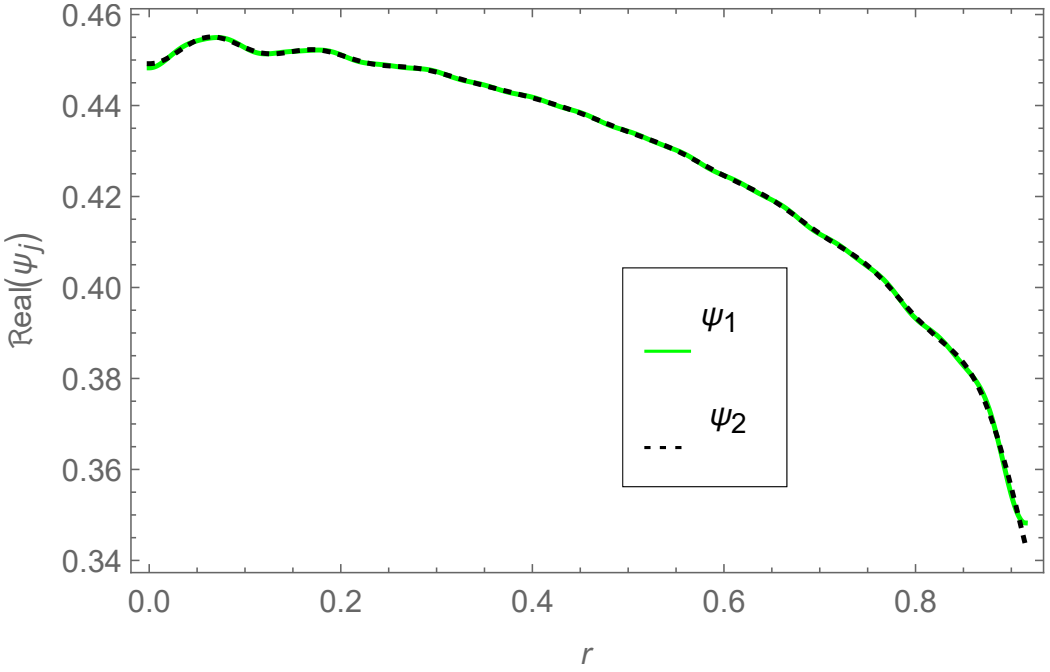

Figure 4.2: Real parts of pressures $\psi_1(r,0)$ and $\psi_2(r,0)$ plotted against r.

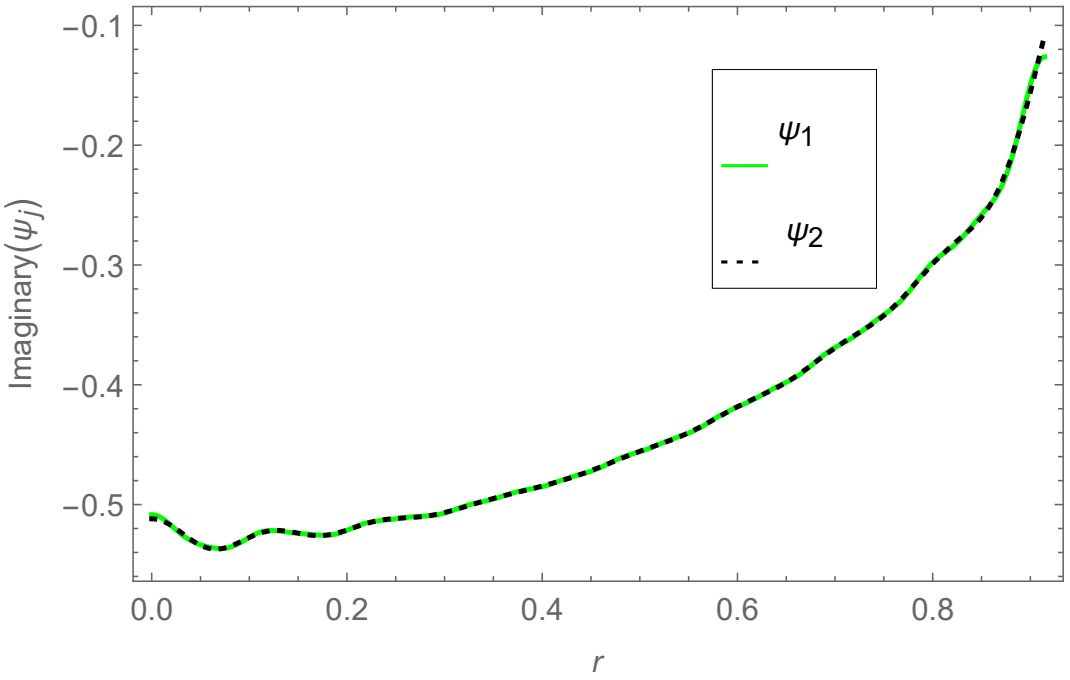

Figure 4.3: Imaginary parts of pressures $\psi_1(r,0)$ and $\psi_2(r,0)$ plotted against r.

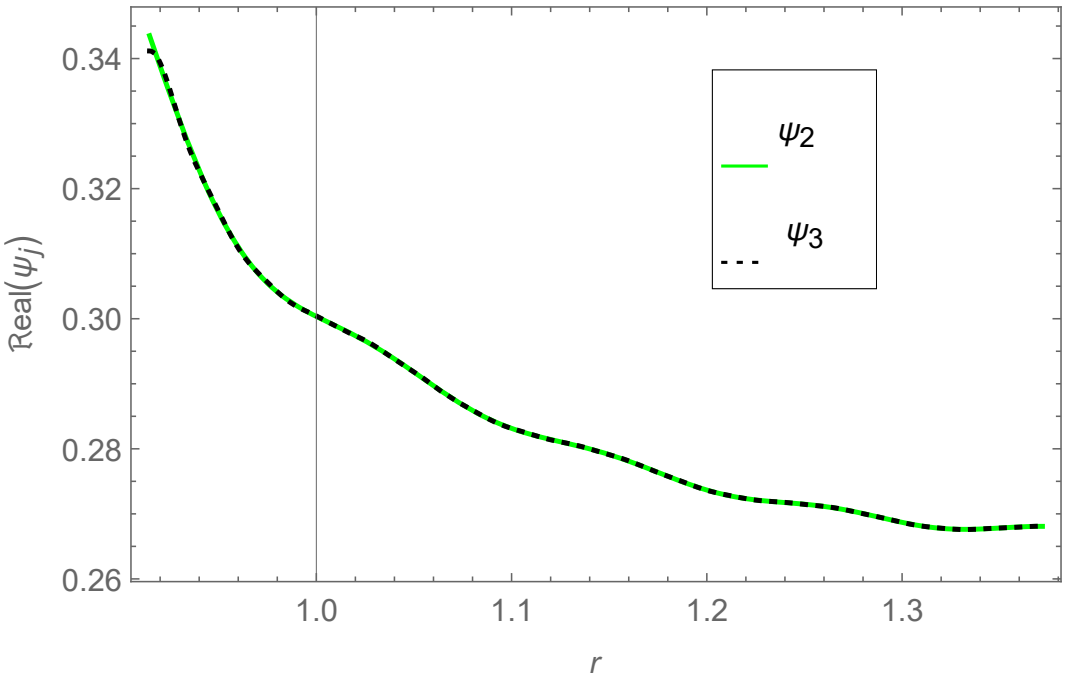

Figure 4.4: Real parts of pressures $\psi_2(r,0)$ and $\psi_3(r,0)$ plotted against r.

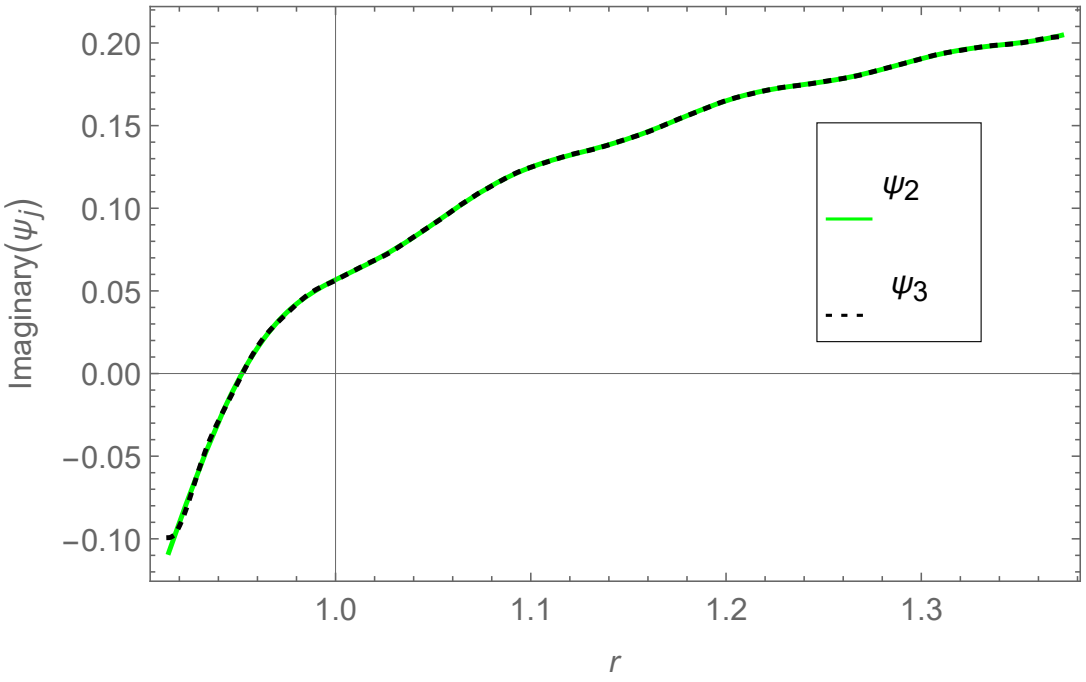

Figure 4.5: Imaginary parts of pressures $\psi_2(r,0)$ and $\psi_3(r,0)$ plotted against r.

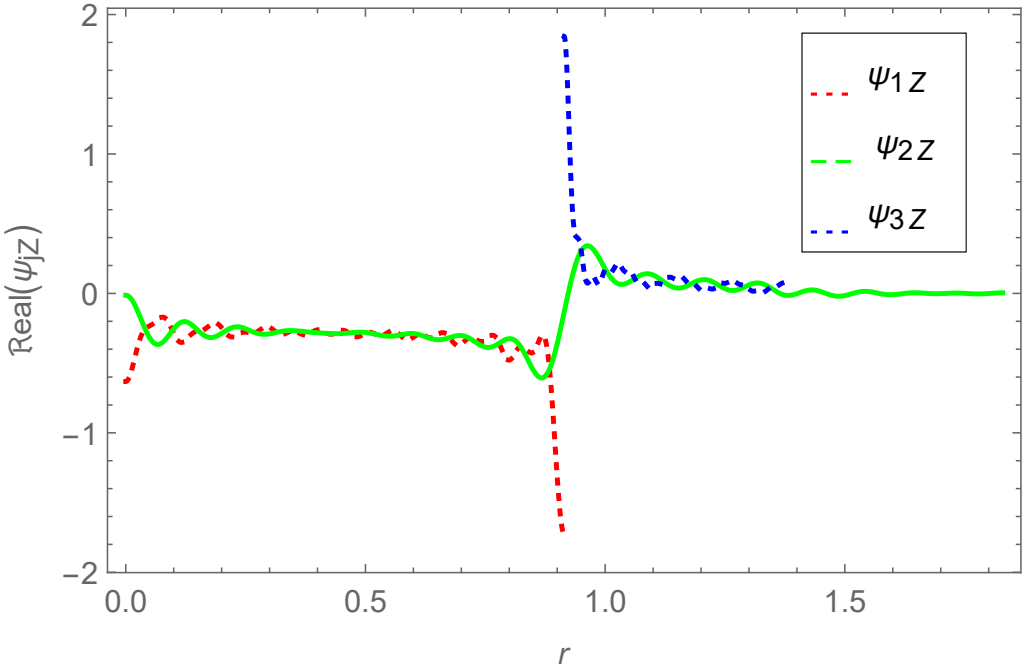

Figure 4.6: Real parts of velocities $\psi_{1z}(r,0)$, $\psi_{2z}(r,0)$ and $\psi_{3z}(r,0)$ plotted against r.

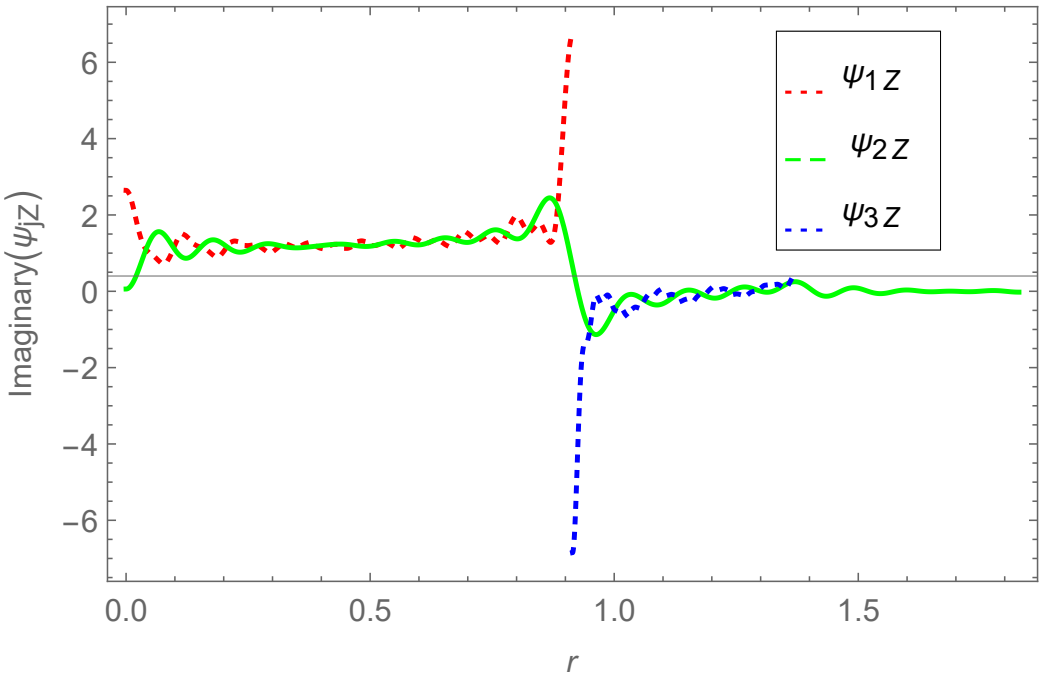

Figure 4.7: Imaginary parts of velocities $\psi_{1z}(r,0)$, $\psi_{2z}(r,0)$ and $\psi_{3z}(r,0)$ plotted against r.

Furthermore, the accuracy of truncated solution can be confirmed through energy flux identity. The power components against frequency are plotted in Figures 4.8-4.9 for circular regions of radii $\bar{a} = 0.1m$, $\bar{b} = 0.15m$ and $\bar{d} = 0.2m$. The roots of involving parameters remain invariant as discussed in the start of this section.

Note that in Figure 4.8 the step-discontinuity is assumed. For the dispersion of energy flux, we plot the reflected and transmitted energy flux against frequency. Moreover, the sum of the scattering power propagation in different regions is unity which justifies the conserved power identity (4.41). In this way the confirmation of matching conditions and conserved power identity validation the truncated solution.

The physical behavior depicted in Figure 4.8, shows that the reflected power in region R_1 increases continuously in frequency regime $1Hz \leq f \leq 1050Hz$. After that, it goes on decreasing and start fluctuating to reaches its minimum for higher frequencies. When the reflected power goes on decreasing then the transmitted power goes on increasing. So that, the reflected and transmitted powers are converse to each other.

In Figure 4.9 the step-discontinuity is removed by taking $b = d$, when an fundamental mode becomes propagating then both the reflected and transmitted powers behave smoothly in frequency regime $1Hz \leq f \leq 1400Hz$. At $f \leq 1400Hz$, the reflection of energy flux increases and transmission decreases.

The power components against frequency plotted in Figures 4.10-4.11 for circular regions $\bar{a} = 0.05m$, $\bar{b} = 0.1m$ and $\bar{d} = 0.2m$. In Figure 3.10 the step-discontinuity is assumed. Furthermore in Figures $4.12-4.13$ the dimensions are fixed as $\bar{a} = 0.2m$, $\bar{b} = 0.25m$ and $\bar{d} = 0.35m$.

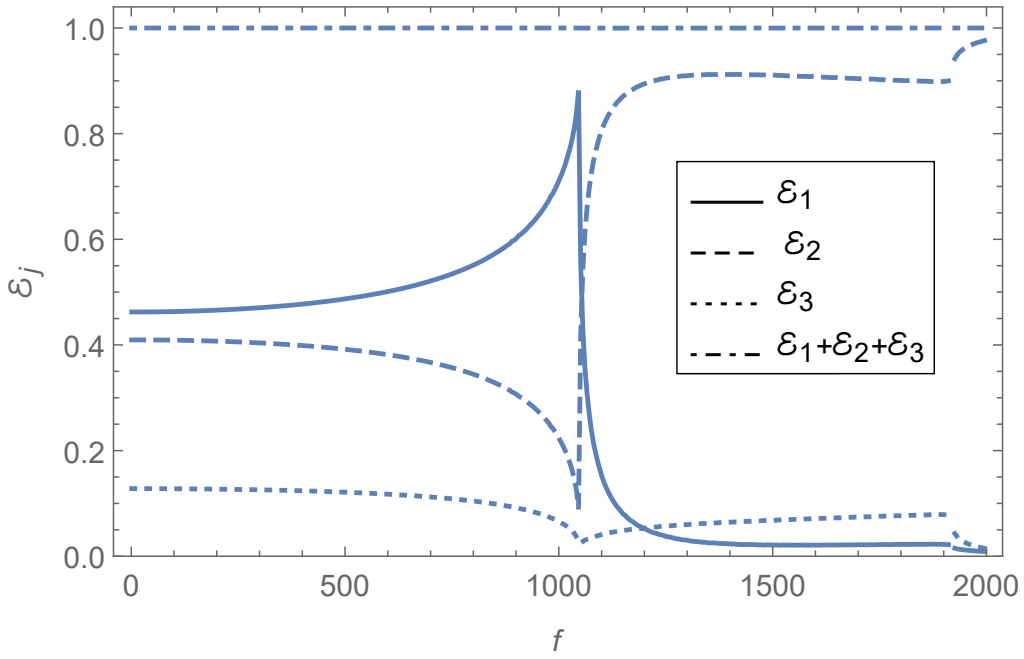

Figure 4.8: Scattered energy flux (ε_j) in regions R_j verses frequency for rigid bounding walls with $\bar{d} > \bar{b}$, where $\bar{a} = 0.1m$, $\bar{b} = 0.15m$, $\bar{d} = 0.2m$ and $N = 20$.

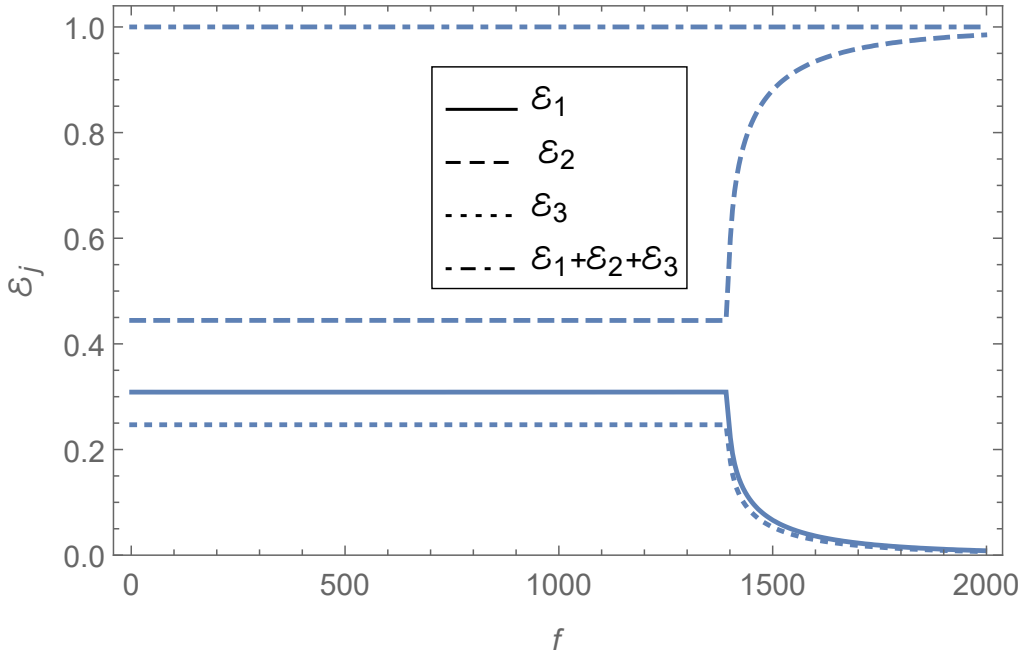

Figure 4.9: Scattered energy fiux (ε_j) in regions R_j verses frequency for rigid bounding walls with $\bar{b} = \bar{d}$, where $\bar{a} = 0.1$, $\bar{b} = 0.15$, $\bar{d} = 0.15$ and $N = 20$.

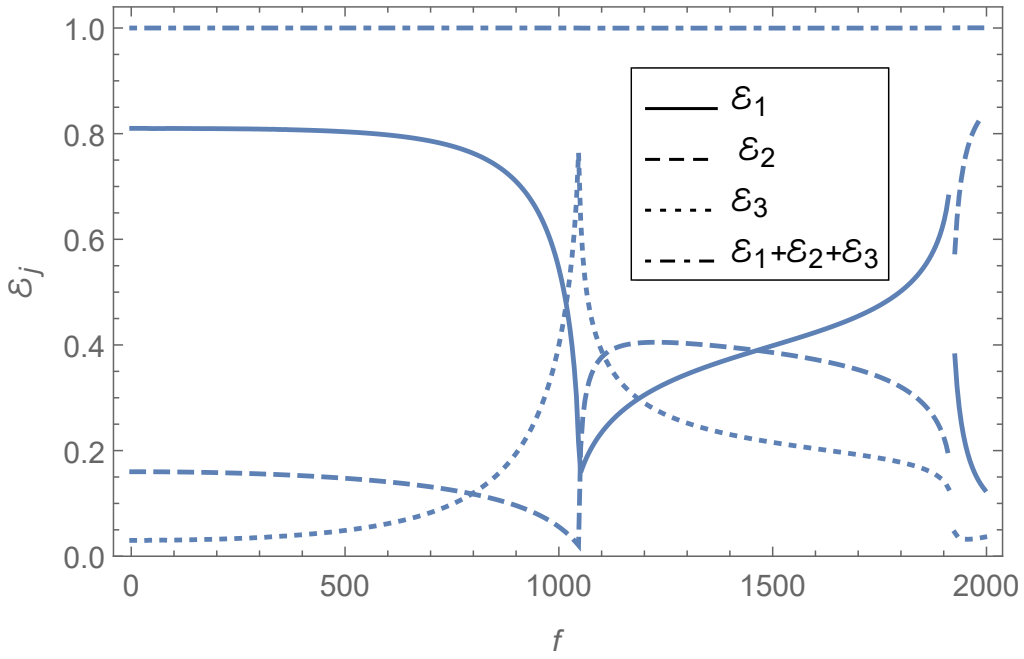

Figure 4.10: Scattered energy flux (ε_j) in regions R_j verses frequency for rigid bounding walls with $\bar{d} > \bar{b}$, where $\bar{a} = 0.05m$, $\bar{b} = 0.1m$, $\bar{d} = 0.2m$ and $N = 20$.

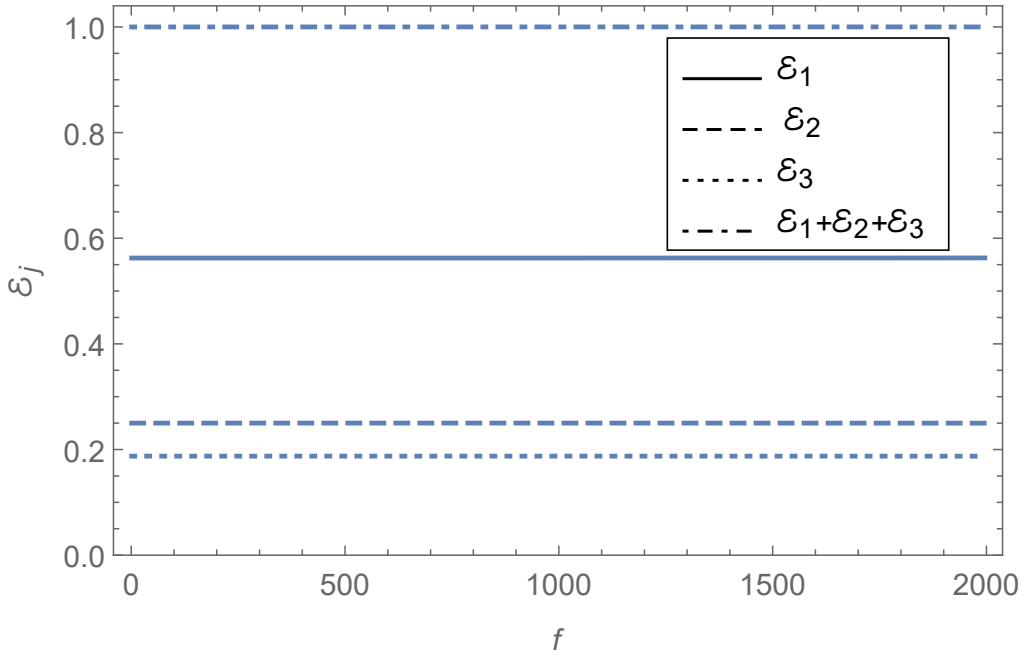

Figure 4.11: Scattered energy flux (ε_j) in regions R_j verses frequency for rigid bounding walls with $\bar{d} = \bar{b}$, where $\bar{a} = 0.05m$, $\bar{b} = 0.1m$, $\bar{d} = 0.1m$ and $N = 20$.

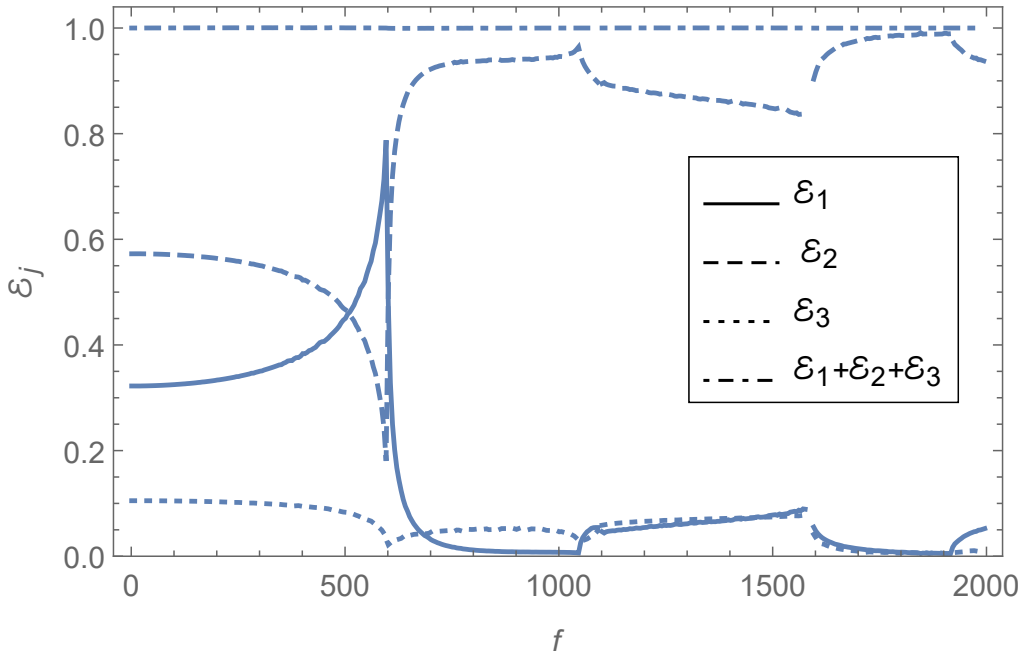

Figure 4.12: Scattered energy flux (ε_j) in regions R_j verses frequency for rigid bounding walls $\bar{d} > \bar{b}$, where $\bar{a} = 0.2m$, $\bar{b} = 0.25m$, $\bar{d} = 0.35m$ and $N = 20$.

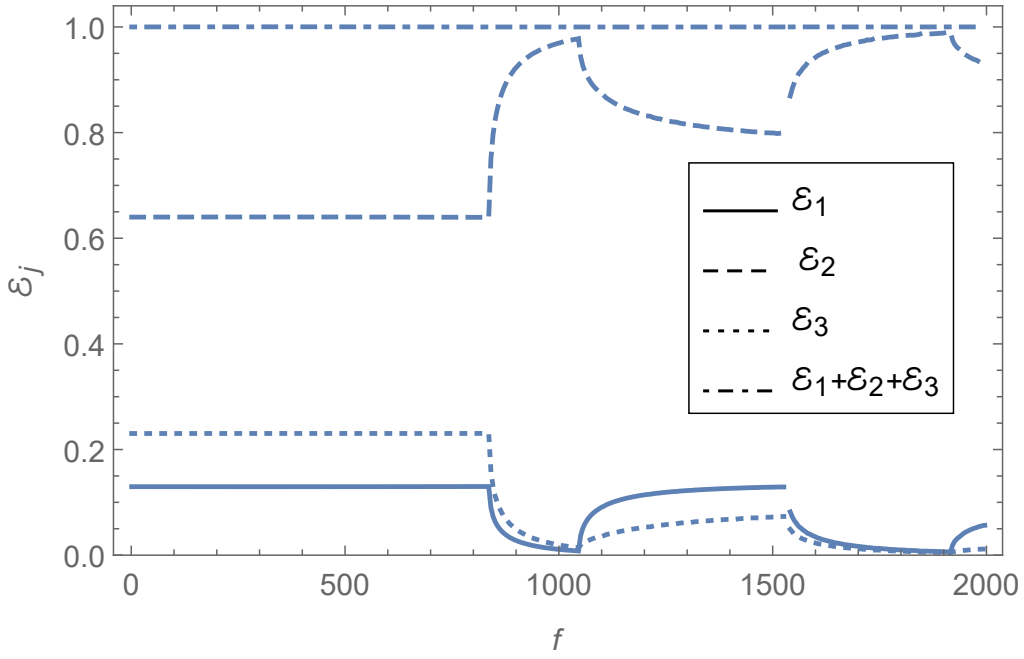

Figure 4.13: Scattered energy flux (ε_j) in regions R_j verses frequency for rigid bounding walls with $\bar{d} = \bar{b}$, where $\bar{a} = 0.2m$, $\bar{b} = 0.25m$, $\bar{d} = 0.25m$ and $N = 20$.

Chapter 5

Summary and Conclusions

In this thesis, the reflection and transmission of acoustics waves in the bifurcated cylindrical waveguides are discussed. Chapter -3 includes a bifurcated cylindrical waveguide bounded by acoustically rigid boundaries along with circular step-discontinuity at interface. Whereas, in Chapter -4 one duct is considered to be an elastic shell instead of rigid duct. The inside of waveguides contains compressible fluid. The incident field is assumed from the central region of the waveguide and its scattering is analyzed. The Mode-Matching solution is developed to discussed the acoustics scattering in the waveguide. The eigenvalues of respective regions and the corresponding eigenfunctions are sorted first to write the eigen expansion form of field potentials. These field potentials involve unknown amplitudes which are found through the matching conditions. The matching conditions together with appropriate orthogonal characteristics help to recaust the differential system into a system of infinite linear algebraic equations. This system is truncated and solved through inversion. The scattering energy flux in each duct is calculated analytically and then is plotted numerically by using the truncated form of solution. It is seen that the truncated form of solution satisfies the conserve power identity accurately. Moreover, it reconstructs the matching conditions at interface. In this way the Mode-Matching solution in truncated form is validated physically and mathematically.

From the mathematical and physical observations of both the problems, the following points are noticeable:

- The eigenvalues and eigenfunctions depend upon the bounding wall conditions of the physical problem. Chapter-3, which contains all rigid boundaries are real and periodic. The corresponding eigenfunctions are orthogonal and undergoes in Strurm-Liouville category. Chapter-4, for elastic shell boundaries the eigenvalues are real, imaginary or complex. The corresponding eigenfunctions are non-orthogonal and undergoes in non-Strurm-Liouville category. Nevertheless, the generalized orthogonality characteristics lead to accurate solution of the problem.

- The power reflection and power transmission depend upon the bounding conditions and structural discontinuities: Chapter-3 the reflection is greater than Chapter-4, whereas the power is also along the boundaries transferring. The involvement of structural discontinuities increases the reflected power. Since more reflected power in discontinuous case than planar in both Chapter-3 and Chapter-4 is observed.

Bibliography

[1] A. D. Rawlins, "Radiation of sound from an unflanged rigid cylindrical duct with an acoustically absorbing internal surface," *Proceedings of the Royal Society London Series A*, vol. 361, no. 1704, pp. 65–91, 1978.

[2] A. Büyükaksoy and B. Polat, "A bifurcated waveguide problem," *ARI-An International Journal for Physical and Engineering Sciences*, vol. 51, no. 3, pp. 196–202, 1999.

[3] M. U. Hassan and A. D. Rawlins, "Sound radiation in a planar trifurcated lined duct," *Wave Motion*, vol. 29, no. 2, pp. 157–174, 1999.

[4] A. D. Rawlins, "A bifurcated circular waveguide problem," *IMA journal of applied mathematics*, vol. 54, no. 1, pp. 59–81, 1995.

[5] W. Koch, "Attenuation of sound in multi-element acoustically lined rectangular ducts in the absence of mean flow," *Journal of Sound and Vibration*, vol. 52, no. 4, pp. 459–496, 1977.

[6] A. D. Rawlins, "Wave propagation in a waveguide," *ZAMM-Journal of Applied Mathematics and Mechanics/Zeitschrift für Angewandte Mathematik und Mechanik: Applied Mathematics and Mechanics*, vol. 83, no. 5, pp. 333–343, 2003.

[7] A. Demír and A. Büyükaksoy, "Wiener–hopf approach for predicting the transmission loss of a circular silencer with a locally reacting lining," *International journal of engineering science*, vol. 43, no. 5-6, pp. 398–416, 2005.

[8] B. Nilsson and O. Brander, "The propagation of sound in cylindrical ducts with mean flow and bulk-reacting lining i. modes in an infinite duct," *IMA Journal of Applied Mathematics*, vol. 26, no. 3, pp. 269–298, 1980.

[9] ——, "The propagation of sound in cylindrical ducts with mean flow and bulk-reacting lining: iii. step discontinuities," *IMA Journal of Applied Mathematics*, vol. 27, no. 1, pp. 105–132, 1981.

[10] ——, "The propagation of sound in cylindrical ducts with mean flow and bulk-reacting lining ii. bifurcated ducts," *IMA Journal of Applied Mathematics*, vol. 26, no. 4, pp. 381–410, 1980.

[11] ——, "The propagation of sound in cylindrical ducts with mean flow and bulk-reacting lining iv. several interacting discontinuities," *IMA Journal of Applied Mathematics*, vol. 27, no. 3, pp. 263–290, 1981.

[12] M. U. Hassan, "Wave scattering by soft-hard three spaced waveguide," *Applied Mathematical Modeling*, vol. 38, pp. 4528–4537, 2014.

[13] M. U. Hassan, M. Meylan, A. Bashir, and M. Sumbul, "Mode-matching analysis for wave scattering in triple and pentafurcated spaced ducts," *Mathematical Methods Applied Sciences*, vol. 39, pp. 3043–3057, 2016.

[14] M. U. Hassan, N. Mahvish, and R. Nawaz, "Reflected field analysis of soft-hard pentafurcated waveguide," *Advances in Mechanical Engineering*, vol. 9, pp. 1–11, 2017.

[15] M. Afzal, R. Nawaz, M. Ayub, and A. Wahab, "Acoustic scattering in flexible waveguide involving step discontinuity," *PloS one*, vol. 9, no. 8, p. e103807, 2014.

[16] R. Nawaz, M. Afzal, and M. Ayub, "Acoustic propagation in two-dimensional waveguide for membrane bounded ducts," *Communications in Nonlinear Science and Numerical Simulation*, vol. 20, no. 2, pp. 421–433, 2015.

[17] M. Afzal, R. Nawaz, and A. Ullah, "Attenuation of dissipative device involving coupled wave scattering and change in material properties," *Applied Mathematics and Computation*, vol. 290, pp. 154–163, 2016.

[18] J. B. Lawrie and M. Afzal, "Acoustic scattering in waveguide with a height discontinuity bridged by a membrane: a tailored galerkin approch," *Journal of Engineering Mathematics*, vol. 105, no. 1, pp. 99–115, 2017.

[19] M. Afzal, M. Ayub, R. Nawaz, and A. Wahab, "Mode-matching solution of a scattering problem in flexible waveguide with abrupt geometric changes," *Imaging, Multi-scale and High Contrast Partial Differential Equations, American Mathematic Society*, vol. 660, pp. 113–129, 2016.

[20] R. Nawaz, M. Afzal, and A. U. Jan, "Fluid-structure coupled wave scattering in a flexible duct at the junction of planar discontinuities," *Advances in Mechanical Engineering*, vol. 9, p. 1687814017713187, 2017.

[21] S. Shafique, M. Afzal, and R. Nawaz, "On mode-matching analysis of fluid-structure coupled wave scattering between two flexible waveguides," *Canadian Journal of Physics*, vol. 95, pp. 581–589, 2016.

[22] T. Nawaz, M. Afzal, and R. Nawaz, "The scattering analysis of trifurcated waveguide involving structural discontinuities," *Advances in Mechanical Engineering*, vol. 11, pp. 1–11, 2019.

[23] J. U. Satti, M. Afzal, and R. Nawaz, "Scattering analysis of a partitioned wave-bearing cavity containing di erent material properties," *Physica Scripta*, vol. 94, no. 11, 2019.

[24] J. B. Lawrie and M. Afzal, "Acoustic scattering in a waveguide with a height discontinuity bridged by a membrane: a tailored galerkin approach," *Journal of Engineering Mathematics*, vol. 105, no. 1, pp. 99–115, 2017.

[25] M. C. Junger and D. Feit, *Sound, structures, and their interaction.* MIT press Cambridge, MA, 1986, vol. 225.

[26] M. Junger and D. Feit, "High-frequency response of point-excited submerged, spherical shells," *The Journal of the Acoustical Society of America*, vol. 45, no. 3, pp. 630–636, 1969.

[27] R. M. Pullen, "Acoustic scattering in circular cylindrical shells: a modal approach based on a generalised orthogonality relation," Ph.D. dissertation, Brunel University London, 2017.

[28] S. S. Rao, *Vibration of continuous systems*. Wiley Online Library, 2007, vol. 464.

[29] L. E. Kinsler, A. R. Frey, A. B. Coppens, and J. V. Sanders, "Fundamentals of acoustics," *Wiley-VCH, 4th Edition*, p. 560, 1999.